

Karpacz, May 16-25, 2024

Correlations, Cluster Formation, and Phase Transitions in Dense Fermion Systems

Gerd Röpke, Rostock



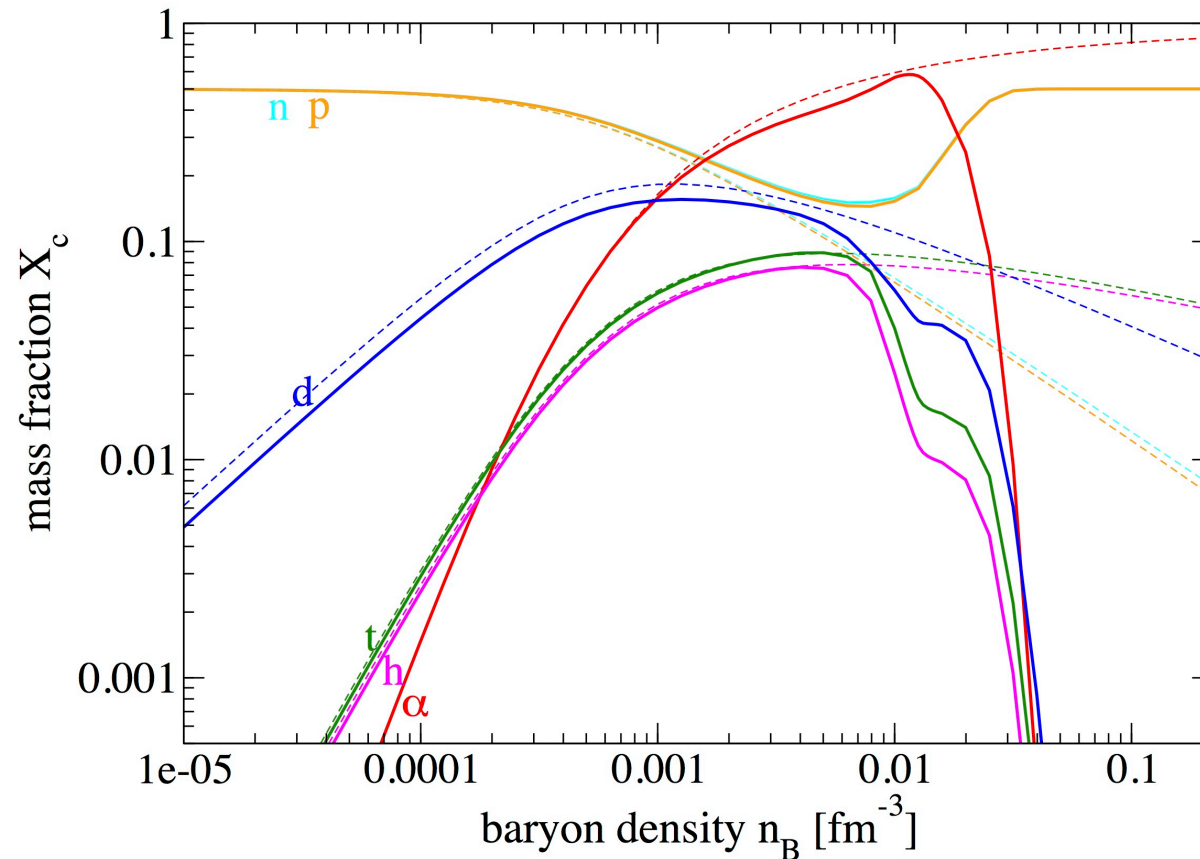
Outlook

- Part I: Quantum statistics and the method of Green functions, Coulomb systems
- Part II: Nuclear systems, correlations, bound states and in-medium effects, equation of state for subsaturation densities
- Part III: phase transitions, pairing and quartetting, nonequilibrium processes and cluster formation, freeze-out concept, heavy-ion collisions, fission, astrophysics
- TI: Green functions and Feynman diagrams, partial summations, self-energy, polarization function, cluster decomposition
- TII: Separable potentials, bound and scattering states, Pauli blocking and shift of the binding energy

EoS including correlations

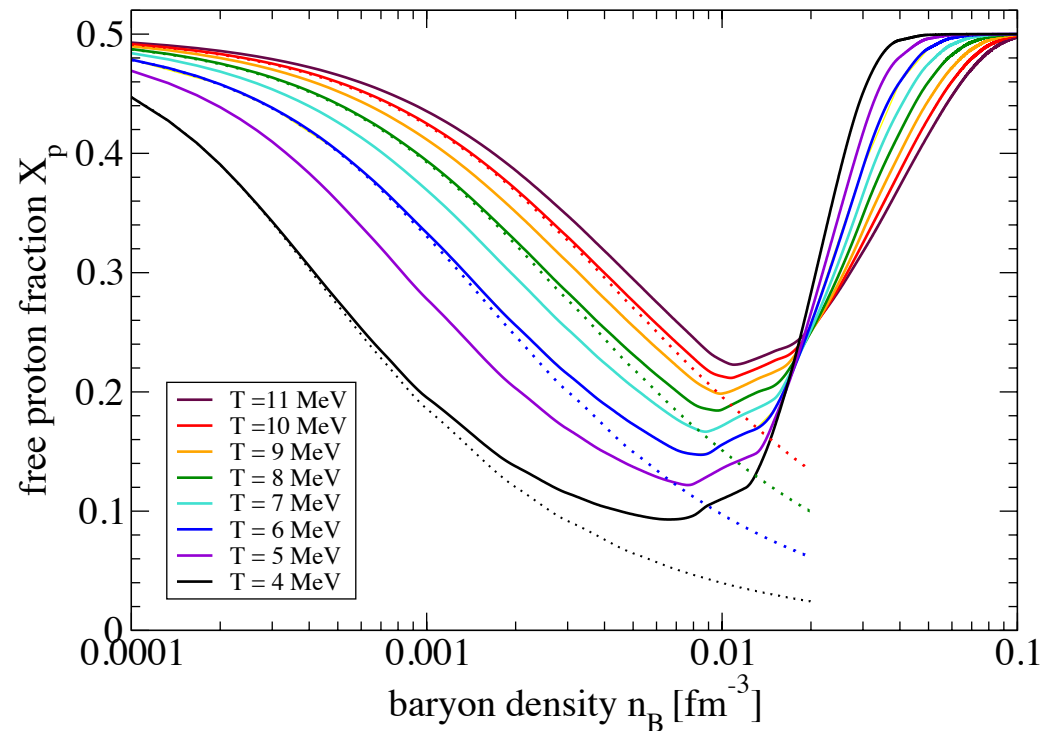
- Composition
- Chemical potential, nuclear matter and stellar matter (β equilibrium)
- Free energy and related quantities, symmetry energy,...
- Phase transition
- Quantum condensates: pairing, quartetting,...

Light Cluster Abundances



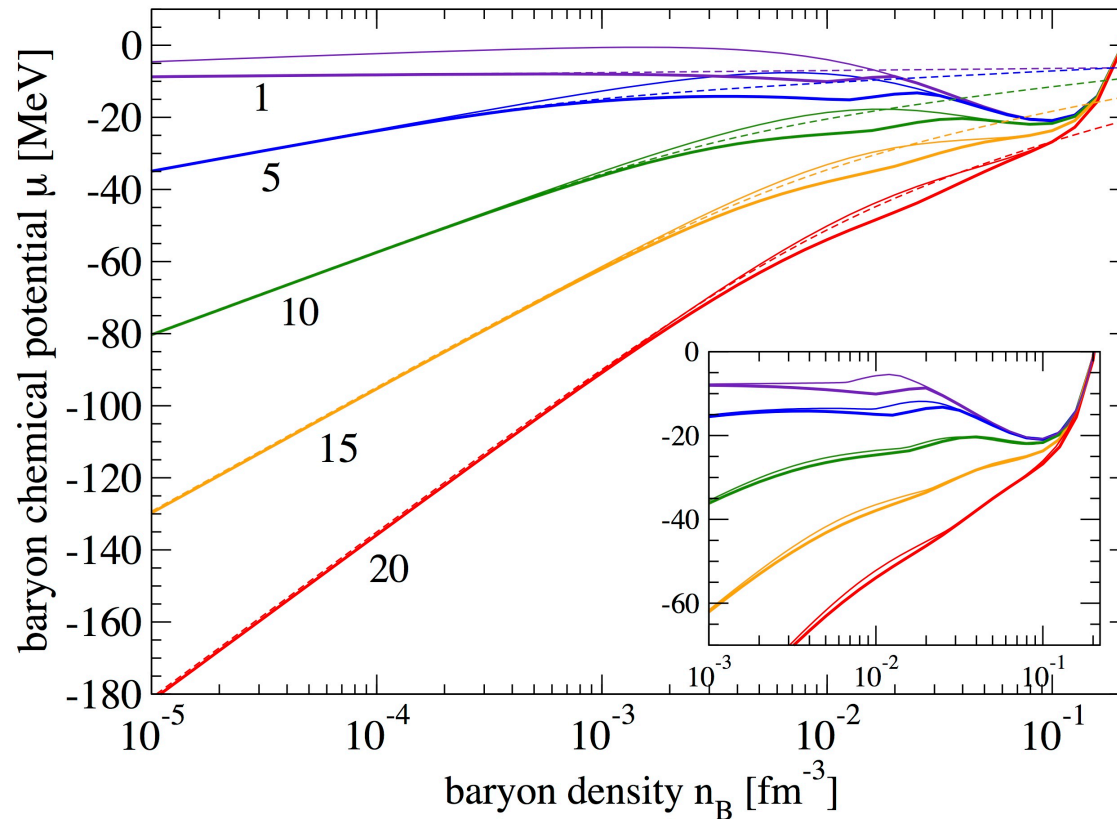
Composition of symmetric matter in dependence on the baryon density n_B , $T = 5$ MeV. Quantum statistical calculation (full) compared with NSE (dotted).

Pauli blocking in symmetric matter



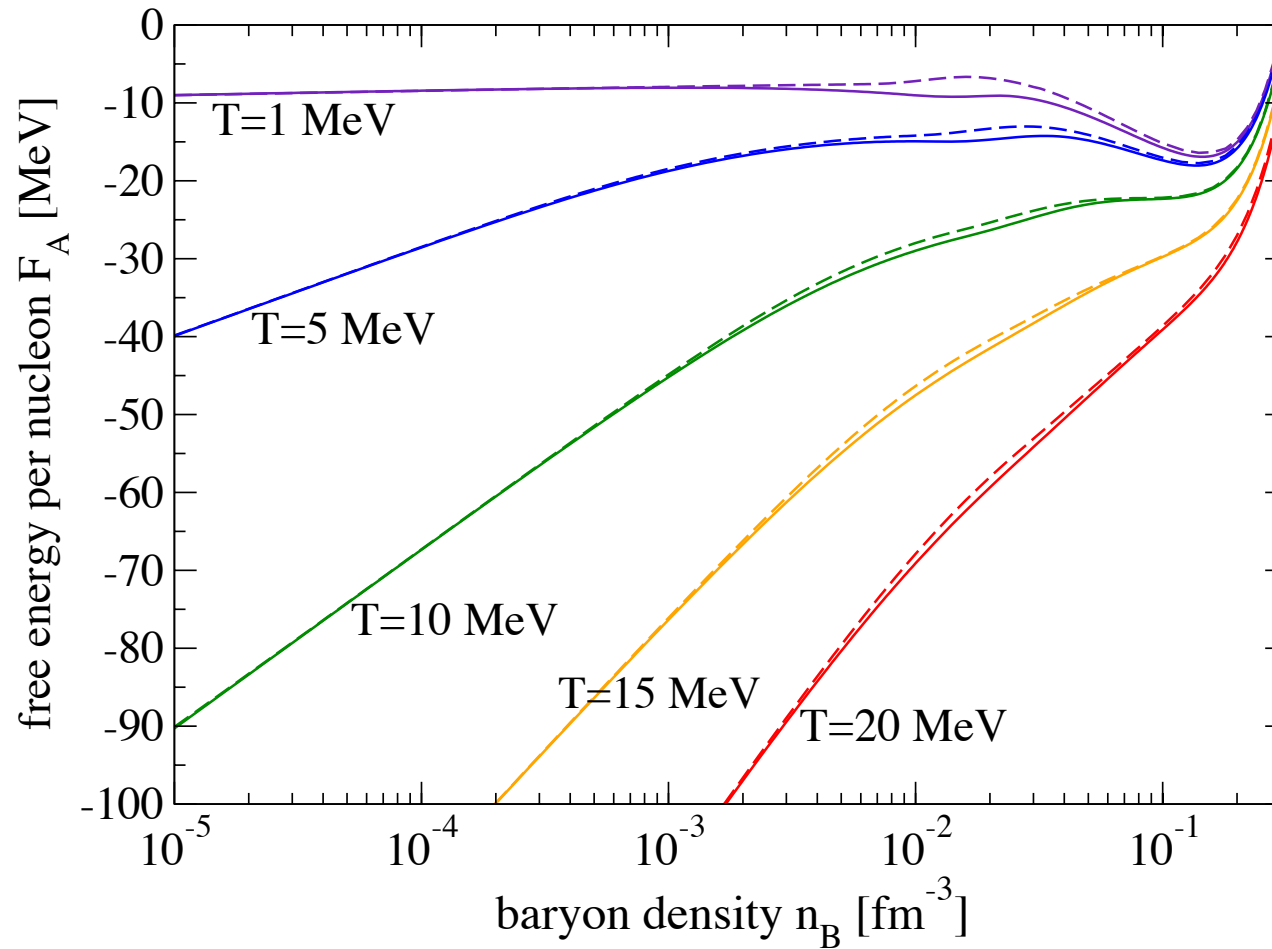
Free proton fraction as function of density and temperature in symmetric matter. QS calculations (solid lines) are compared with the NSE results (dotted lines). **Mott effect** in the region $n_{\text{saturation}}/5$.

Equation of state: chemical potential



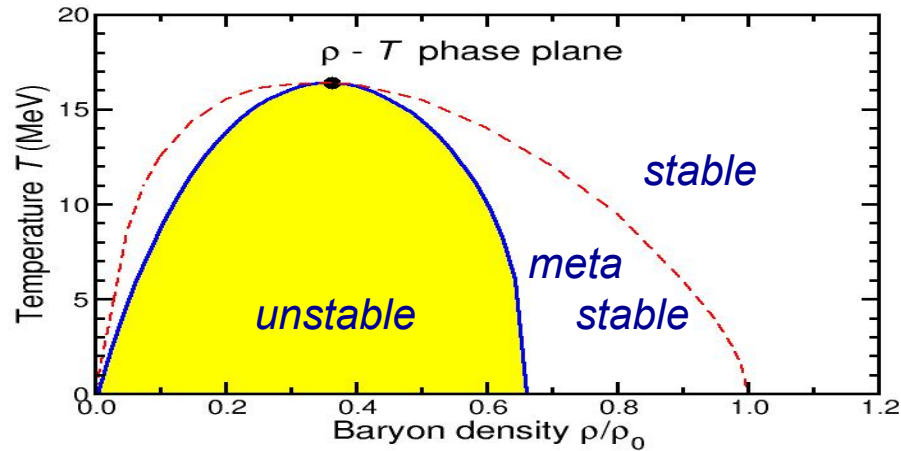
Chemical potential for symmetric matter. $T=1, 5, 10, 15, 20$ MeV.
QS calculation compared with RMF (thin) and NSE (dashed).
Insert: QS calculation without continuum correlations (thin lines).

Symmetric matter: free energy per nucleon



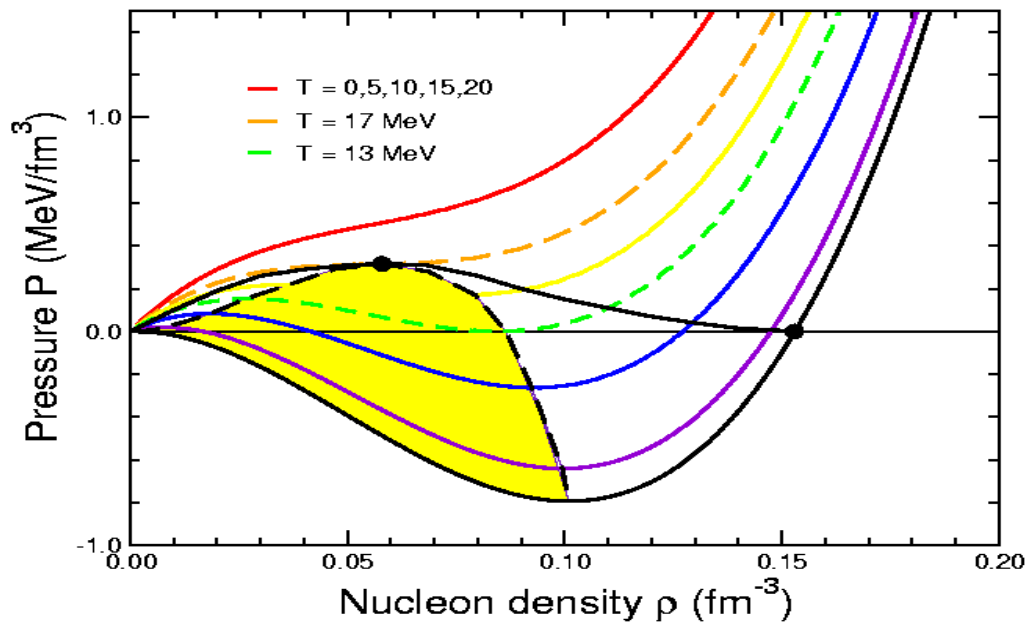
Dashed lines: no **continuum correlations**

Nuclear matter



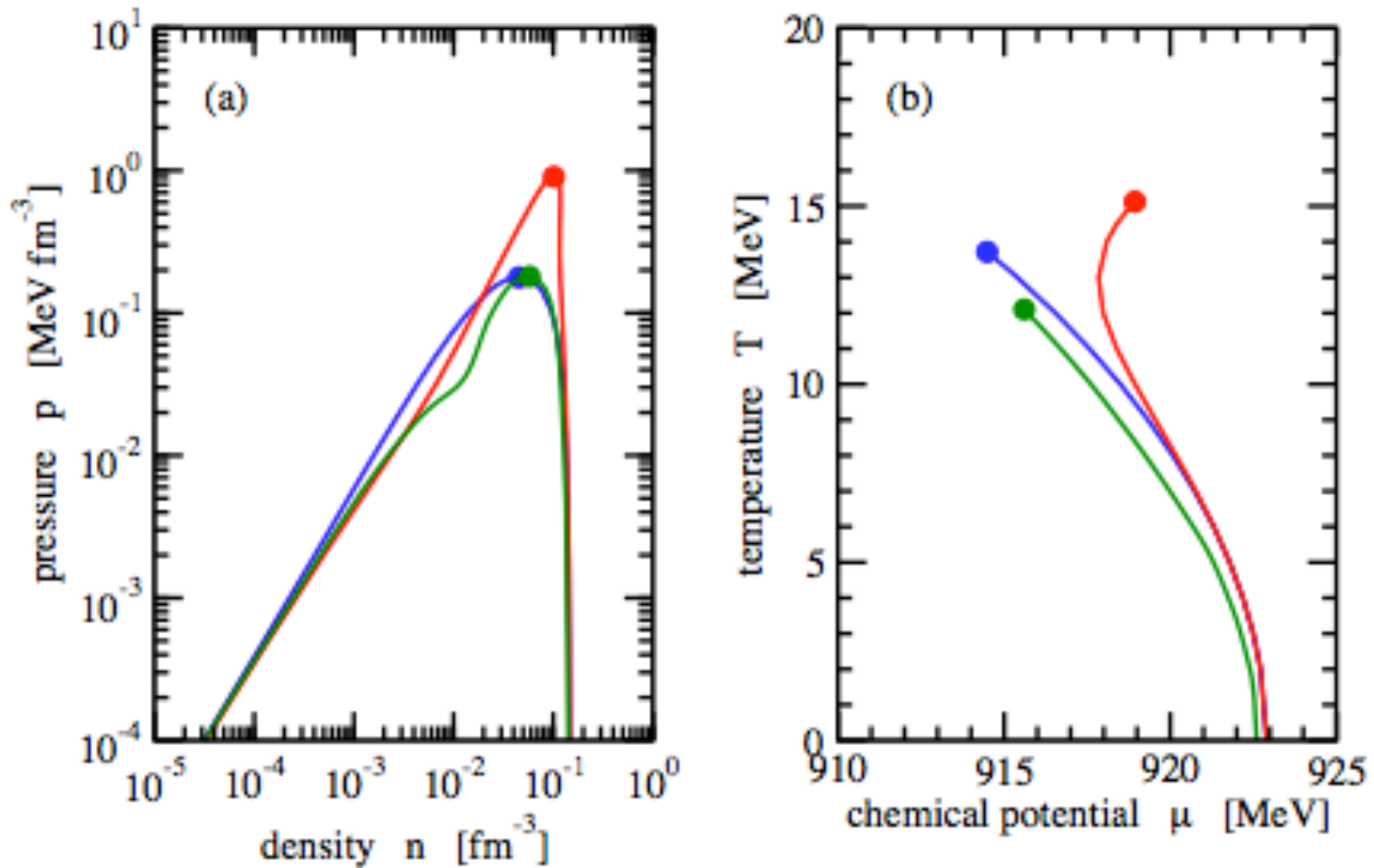
Phase diagram

$$\varepsilon(T; \rho) = \varepsilon_{\text{FG}}(T; \rho) + w(\rho)$$



Equation of state:
 $p_T(\rho)$

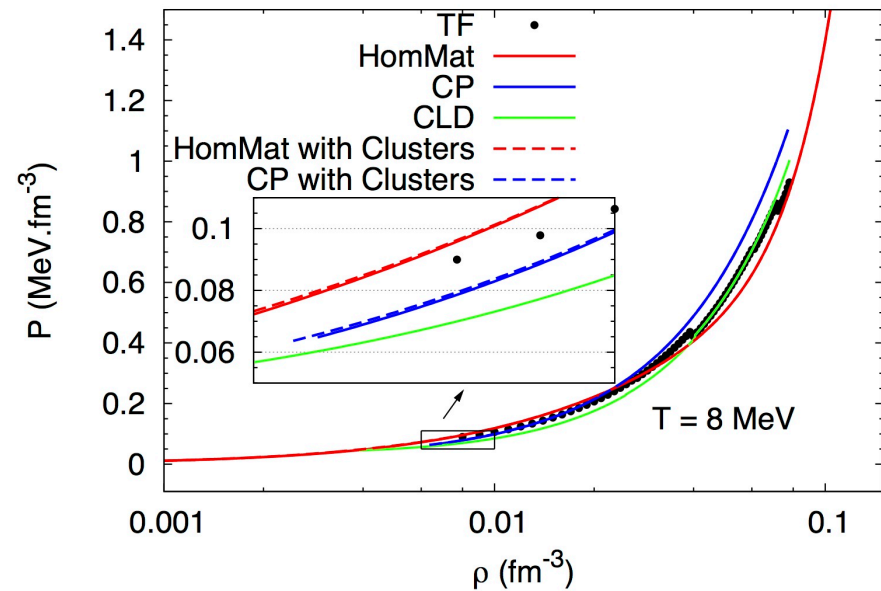
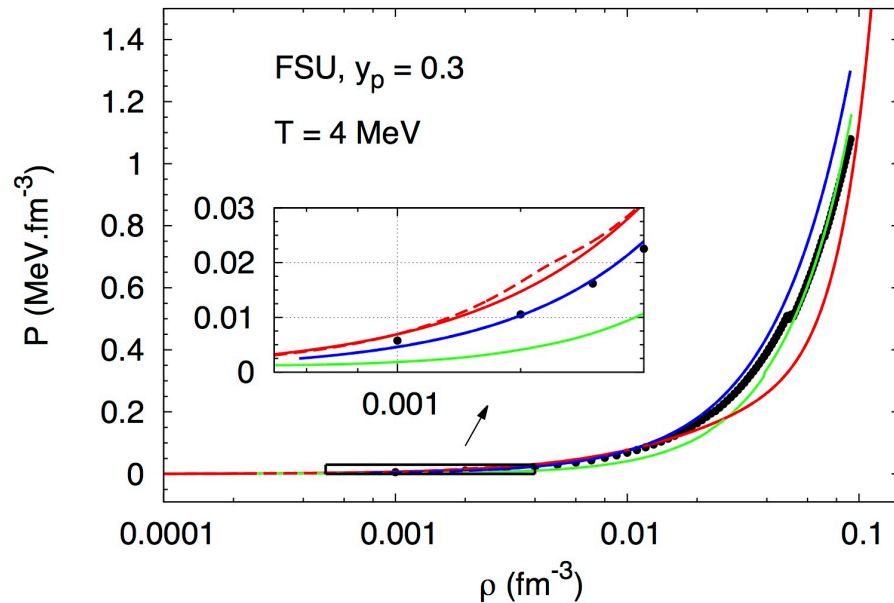
Liquid-vapor phase transition



blue: no light cluster, green: with light clusters, QS, red: cluster-RMF

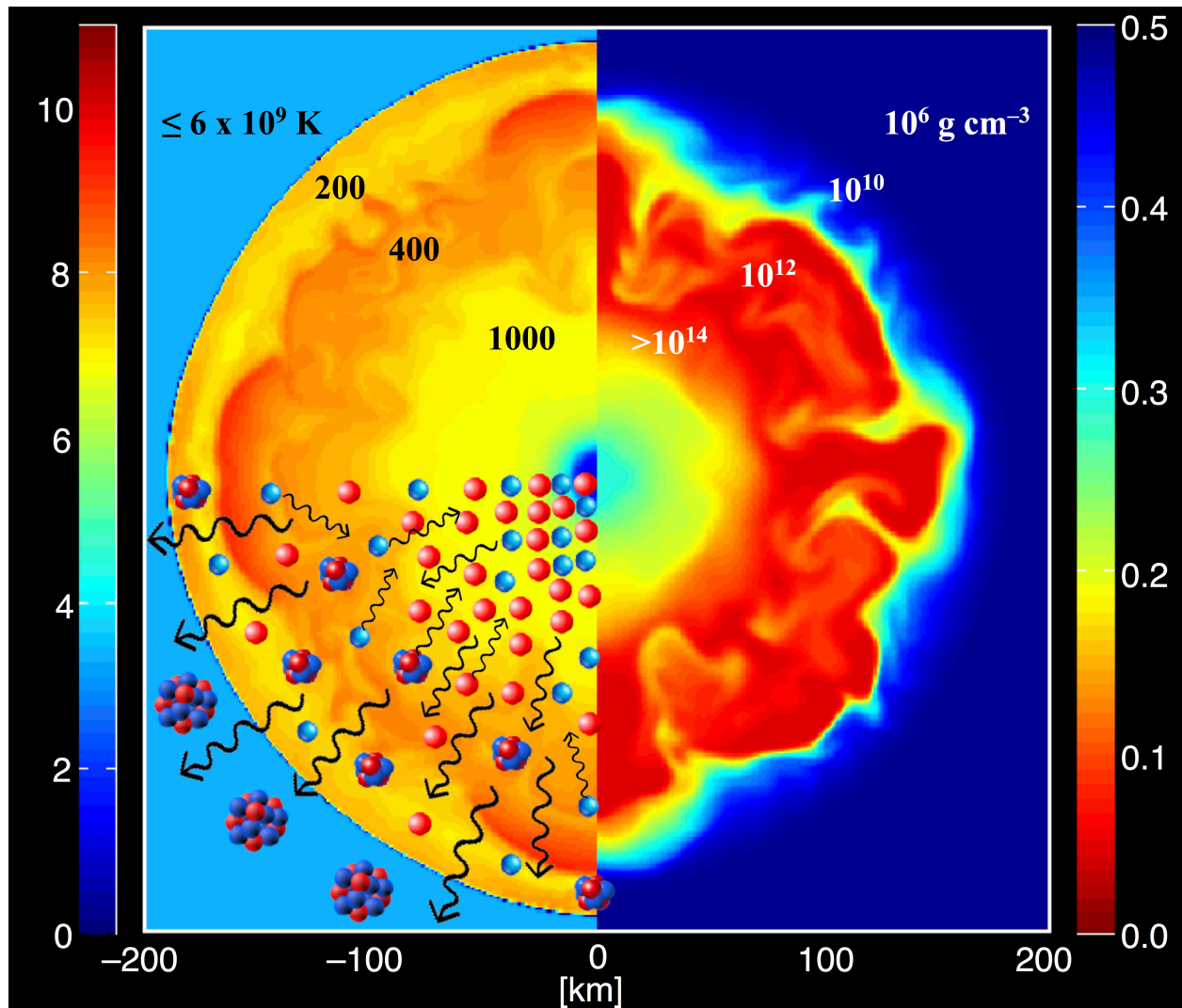
S. Typel et al., PRC 81, 015803 (2010)

Light clusters and pasta phases in core-collapse supernova matter



Pressure as function of density, $Y_p=0.3$, $T=4 \text{ MeV} / 8 \text{ MeV}$.
With and without pasta, including or not clusters. TF - Thomas-Fermi,
CP - coexisting-phases method, CLD - compressible liquid drop

Stellar matter: Supernova explosion



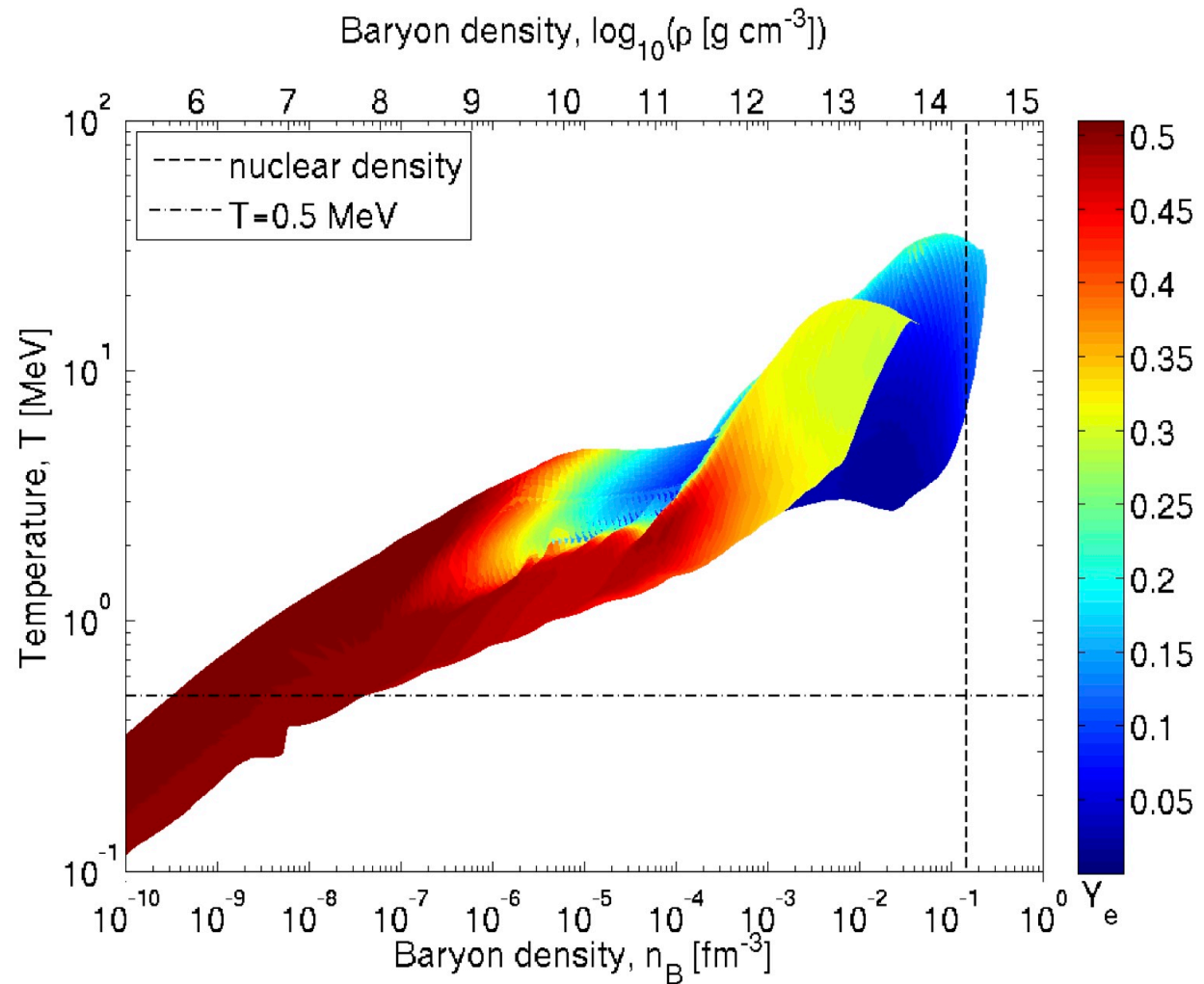
Snapshot:
Temperature,
Density,
Proton fraction,
Entropy,
Neutrino flux
Cluster formation

Simulation by
Tobias Fischer

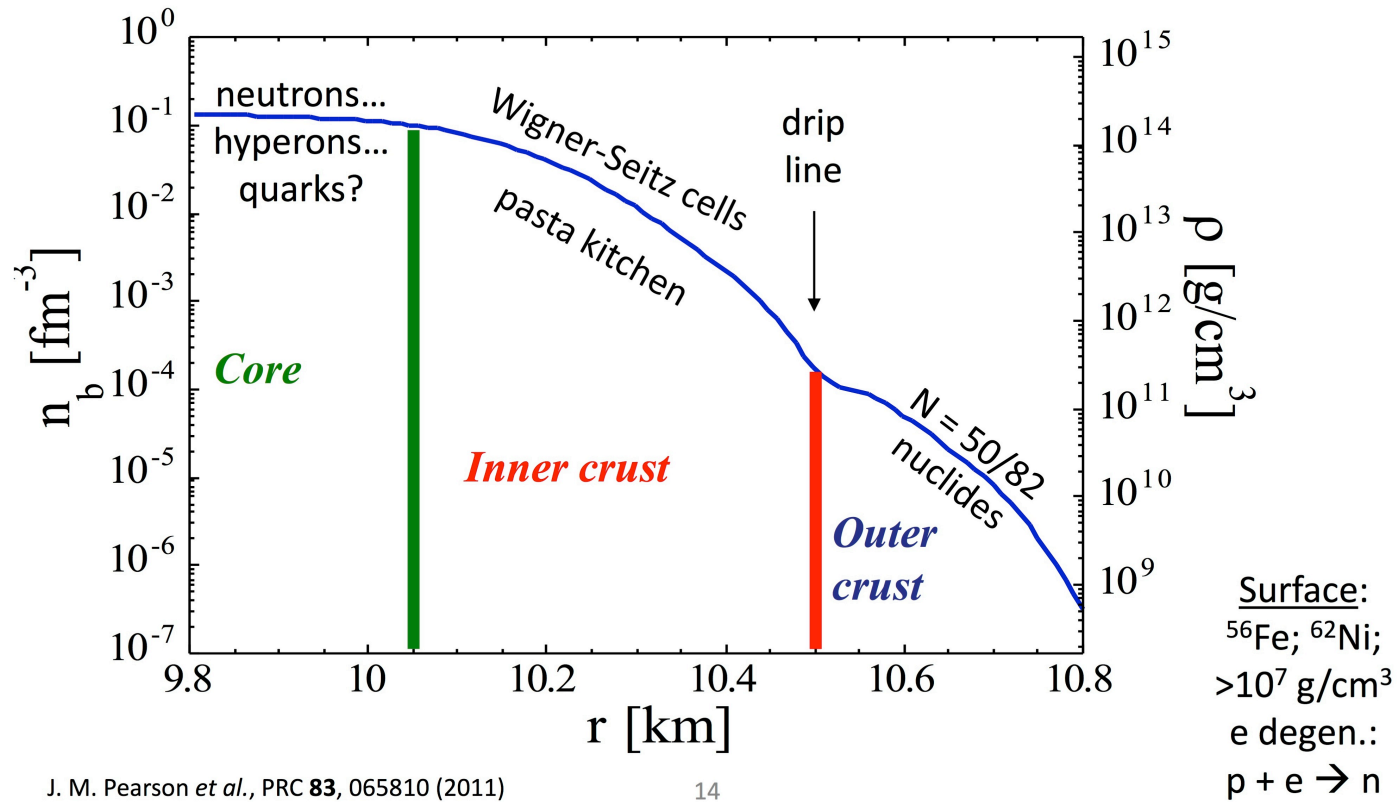
Nuclear matter phase diagram

Exploding
supernova

T. Fischer et al.,
arXiv 1307.6190



Density of neutron star crust

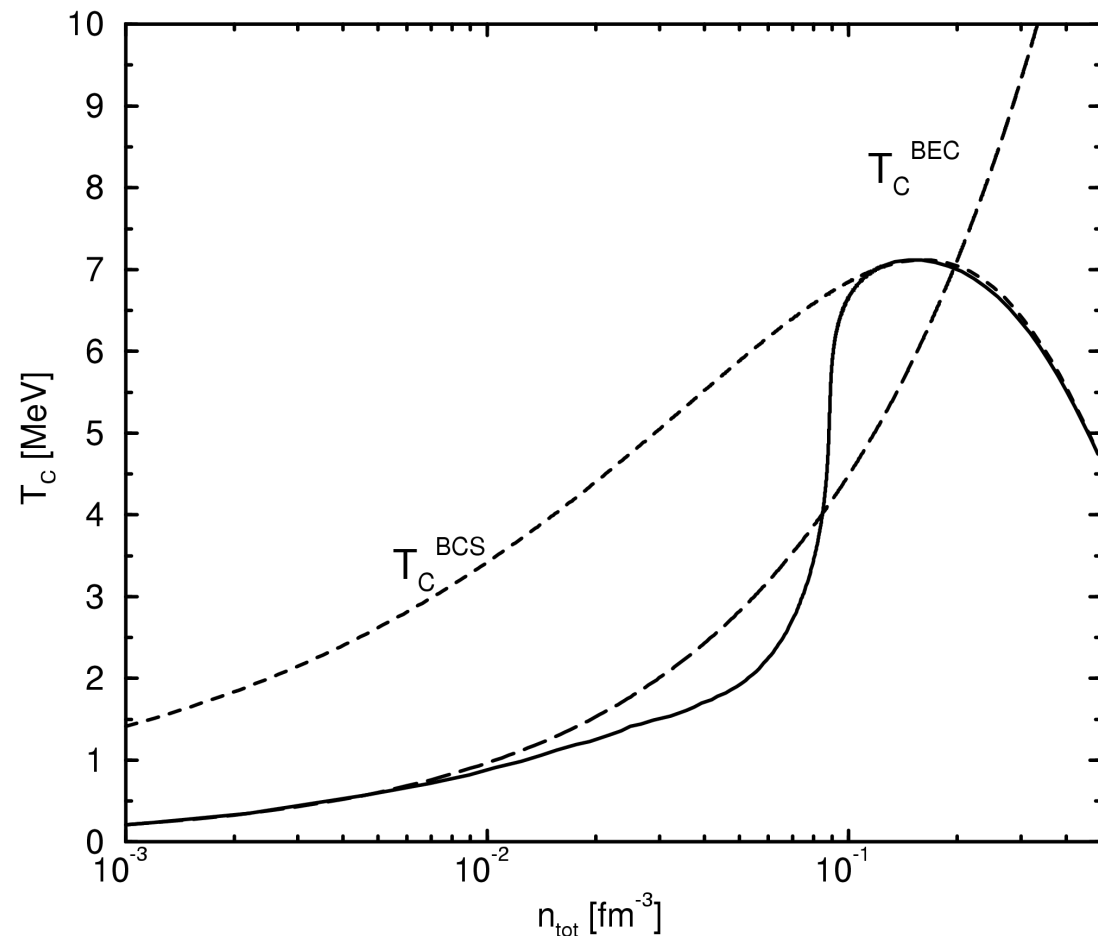


Quantum condensate

Bose-Einstein-
Condensation
of deuterons
(BEC)

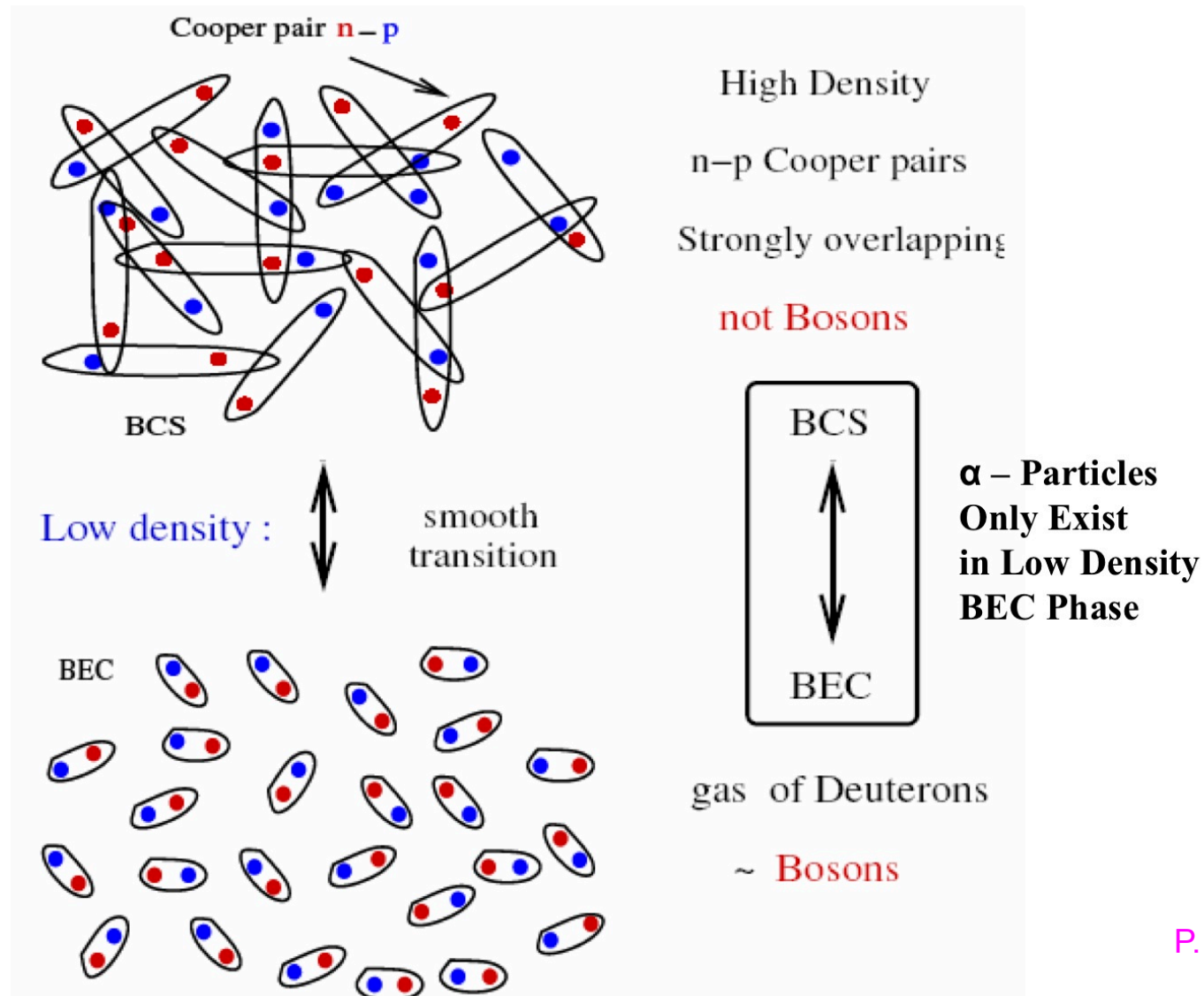
Bardeen-Cooper-
Schrieffer
pairing
(BCS)

below T_c :
grand canonical ρ not valid,
fluctuation: pair amplitude $a_1 a_{-1}$
diagonalization: Bogoliubov



T. Alm *et al.* Z. Phys. A337, 355 (1990)
H. Stein *et al.*, Z. Phys. A351, 259 (1995)
M. Baldo *et al.*, Phys. Rev. C 52, 975 (1995)

Crossover from BEC to BCS pairing



Few-particle Schrödinger equation in a dense medium

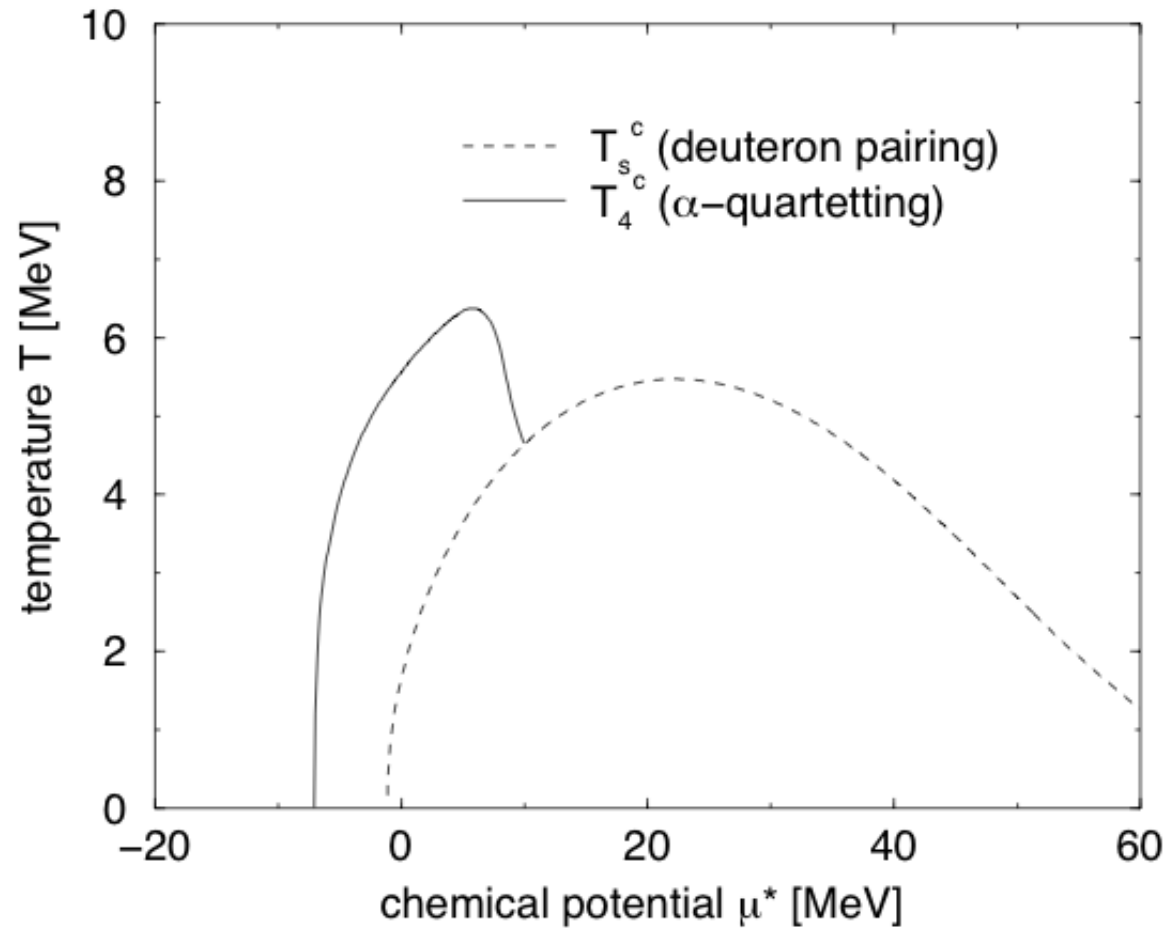
4-particle Schrödinger equation with medium effects

$$\begin{aligned} & \left(\left[E^{HF}(p_1) + E^{HF}(p_2) + E^{HF}(p_3) + E^{HF}(p_4) \right] \right) \Psi_{n,P}(p_1, p_2, p_3, p_4) \\ & + \sum_{p'_1, p'_2} (1 - f_{p_1} - f_{p_2}) V(p_1, p_2; p'_1, p'_2) \Psi_{n,P}(p'_1, p'_2, p_3, p_4) \\ & + \{ \text{permutations} \} \\ & = E_{n,P} \Psi_{n,P}(p_1, p_2, p_3, p_4) \end{aligned}$$

Thouless criterion
for quantum condensate:

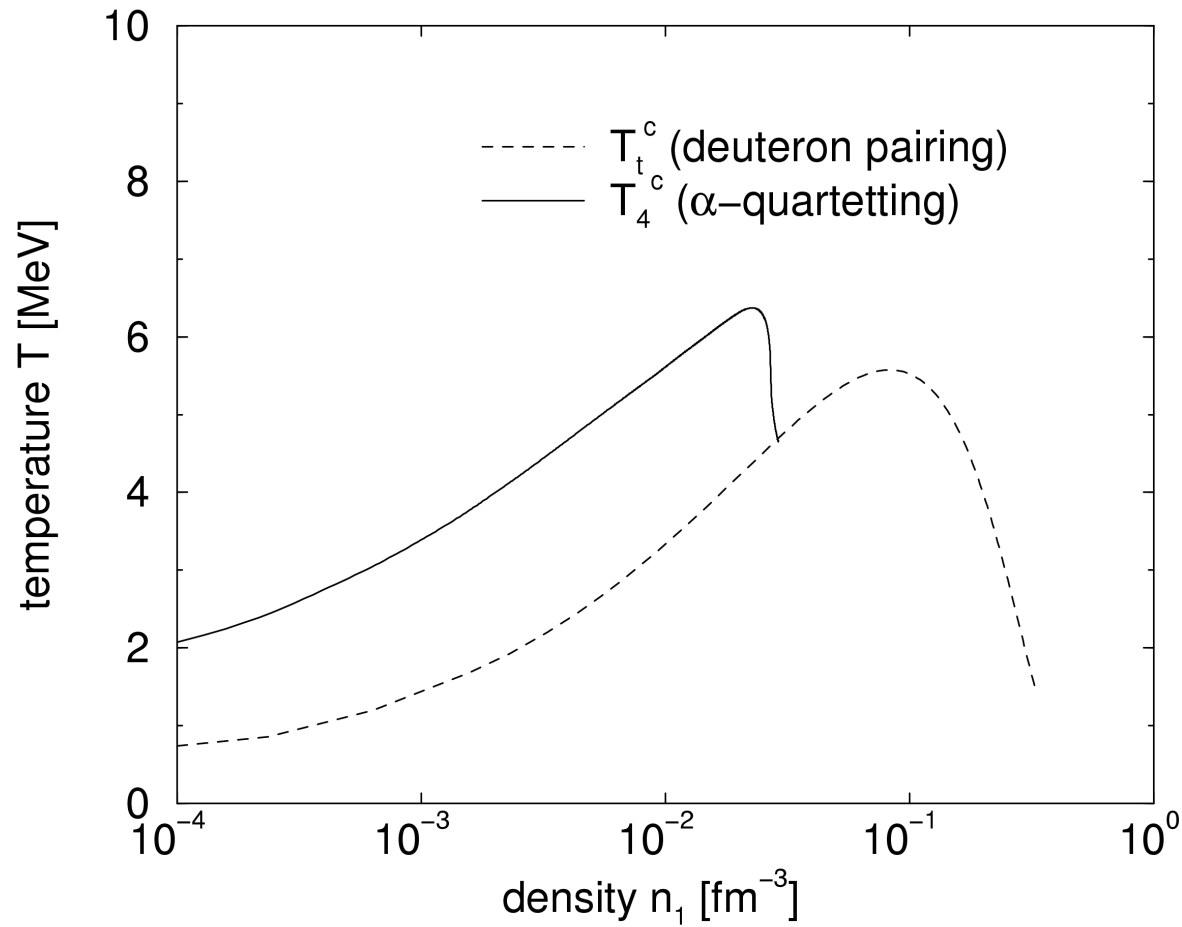
$$E_{n,P=0}(T, \mu) = 4\mu$$

α -cluster-condensation (quartetting)



G.R., A.Schnell, P.Schuck, and P.Nozieres, PRL 80, 3177 (1998)

α -cluster-condensation (quartetting)



G.R., A.Schnell, P.Schuck, and P.Nozieres, PRL 80, 3177 (1998)

The Hoyle state in ^{12}C

^{12}C : from astrophysics: excited state predicted near the 3α threshold energy (F. Hoyle).

a 0^+ state at 0.39 MeV above the 3α threshold energy has been found.

not described by shell structure calculations,
 3α cluster interact predominantly in relative S waves,
gas-like structure, THSR state

A. Tohsaki et al., PRL 87, 192501 (2001)

α -particle condensation in low-density nuclear matter,
 ρ below $\rho_{\text{sat}}/5$

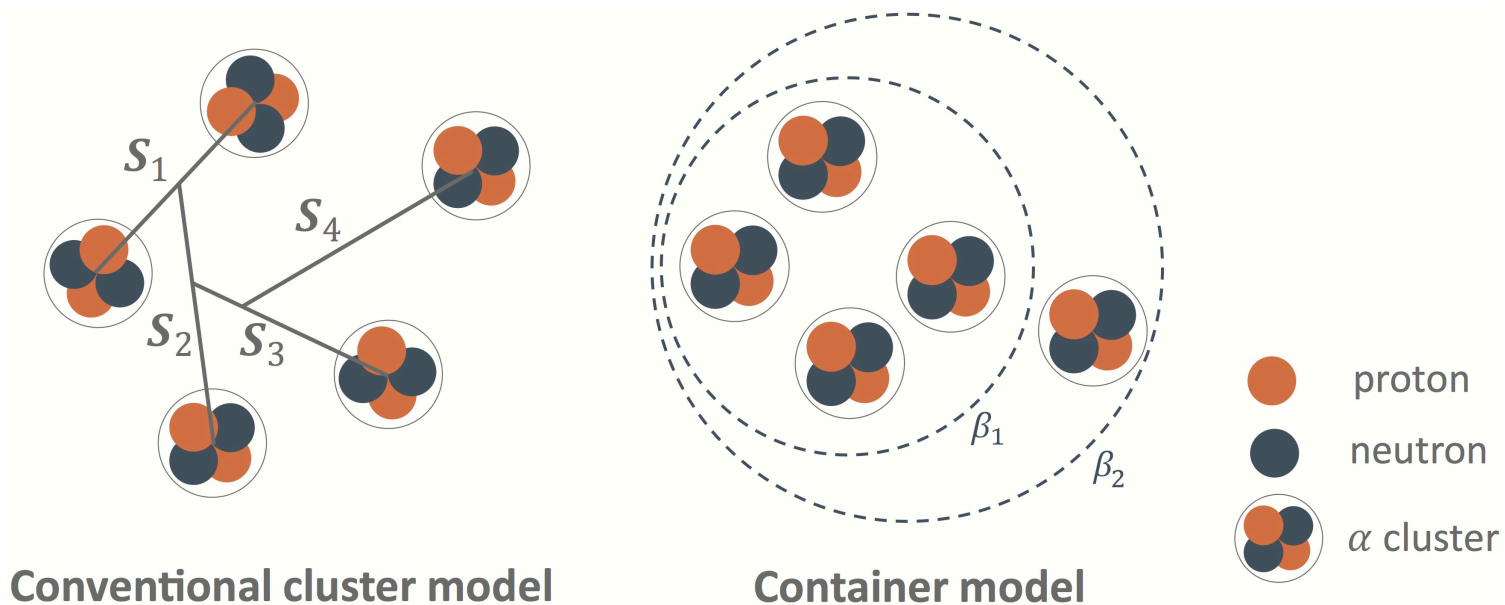
$n\alpha$ nuclei: ^8Be , ^{12}C , ^{16}O , ^{20}Ne , ^{24}Mg , ...

cluster type structures near the $n\alpha$ breakup threshold energy

The 5α condensate state in ^{20}Ne

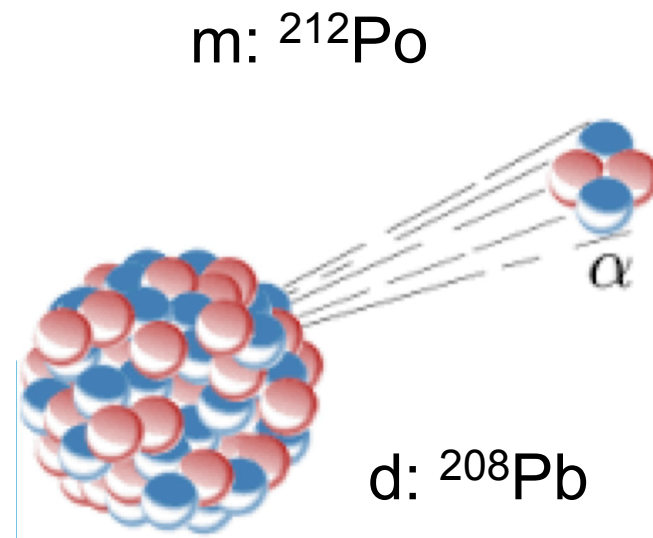
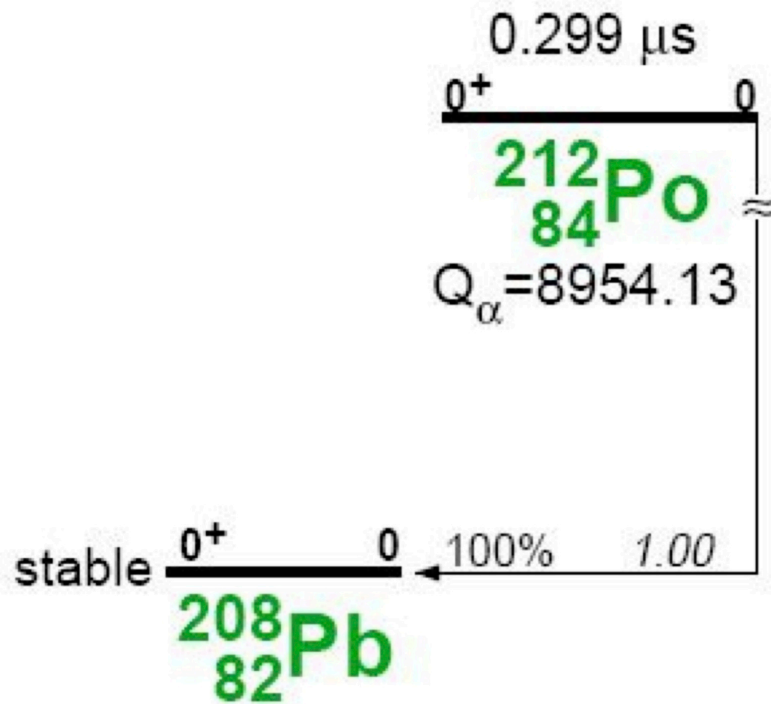
α condensation is a general phenomenon: ^{12}C , ^{16}O , ^{20}Ne , ...

Container picture: B. Zhou et al., Phys. Rev. Lett. 110, 262501 (2013)



B. Zhou, Y. Funki, H. Horiuchi, Y. Ma, G. Ropke, P. Schuck, A. Tohsaki, T. Yamada, Nature Comm. 14, 1 (2023)

Preformation: α decay of ^{212}Po



Clusters in an external potential

c. o. m. coordinate \mathbf{R} , relative coordinates \mathbf{s}_j $\Psi(\mathbf{R}, \mathbf{s}_j) = \varphi^{\text{intr}}(\mathbf{s}_j, \mathbf{R}) \Phi(\mathbf{R})$

normalization $\int dR |\Phi(\mathbf{R})|^2 = 1$ $\int ds_j |\varphi^{\text{intr}}(\mathbf{s}_j, \mathbf{R})|^2 = 1$

N. Gidopoulos, E. Gross (2014)

Wave equation for the c.o.m. motion

$$-\frac{\hbar^2}{2Am} \nabla_{\mathbf{R}}^2 \Phi(\mathbf{R}) - \frac{\hbar^2}{Am} \int ds_j \varphi^{\text{intr},*}(\mathbf{s}_j, \mathbf{R}) [\nabla_{\mathbf{R}} \varphi^{\text{intr}}(\mathbf{s}_j, \mathbf{R})] [\nabla_{\mathbf{R}} \Phi(\mathbf{R})]$$

$$-\frac{\hbar^2}{2Am} \int ds_j \varphi^{\text{intr},*}(\mathbf{s}_j, \mathbf{R}) [\nabla_{\mathbf{R}}^2 \varphi^{\text{intr}}(\mathbf{s}_j, \mathbf{R})] \Phi(\mathbf{R}) + \int dR' W(\mathbf{R}, \mathbf{R}') \Phi(\mathbf{R}') = E \Phi(\mathbf{R})$$

c.o.m. effective potential

$$W(\mathbf{R}, \mathbf{R}') = \int ds_j ds'_j \varphi^{\text{intr},*}(\mathbf{s}_j, \mathbf{R}) [T[\nabla_{\mathbf{s}_j}] \delta(\mathbf{R} - \mathbf{R}') \delta(\mathbf{s}_j - \mathbf{s}'_j) + V(\mathbf{R}, \mathbf{s}_j; \mathbf{R}', \mathbf{s}'_j)] \varphi^{\text{intr}}(\mathbf{s}'_j, \mathbf{R}')$$

Wave equation for the intrinsic motion

$$-\frac{\hbar^2}{Am} \Phi^*(\mathbf{R}) [\nabla_{\mathbf{R}} \Phi(\mathbf{R})] [\nabla_{\mathbf{R}} \varphi^{\text{intr}}(\mathbf{s}_j, \mathbf{R})] - \frac{\hbar^2}{2Am} |\Phi(\mathbf{R})|^2 \nabla_{\mathbf{R}}^2 \varphi^{\text{intr}}(\mathbf{s}_j, \mathbf{R})$$

$$+ \int dR' ds'_j \Phi^*(\mathbf{R}) [T[\nabla_{\mathbf{s}_j}] \delta(\mathbf{R} - \mathbf{R}') \delta(\mathbf{s}_j - \mathbf{s}'_j) + V(\mathbf{R}, \mathbf{s}_j; \mathbf{R}', \mathbf{s}'_j)] \Phi(\mathbf{R}') \varphi^{\text{intr}}(\mathbf{s}'_j, \mathbf{R}') = F(\mathbf{R}) \varphi^{\text{intr}}(\mathbf{s}_j, \mathbf{R})$$

G. R. et al., PRC 90, 034304 (2014)

Quartet wave function

Four-particle wave equation in position space representation

$$[E_4 - \hat{h}_1 - \hat{h}_2 - \hat{h}_3 - \hat{h}_4] \Psi_4(\mathbf{r}_1 \mathbf{r}_2 \mathbf{r}_3 \mathbf{r}_4) = \int d^3 \mathbf{r}'_1 d^3 \mathbf{r}'_2 \langle \mathbf{r}_1 \mathbf{r}_2 | B V_{N-N} | \mathbf{r}'_1 \mathbf{r}'_2 \rangle \Psi_4(\mathbf{r}'_1 \mathbf{r}'_2 \mathbf{r}_3 \mathbf{r}_4) \\ + \int d^3 \mathbf{r}'_1 d^3 \mathbf{r}'_3 \langle \mathbf{r}_1 \mathbf{r}_3 | B V_{N-N} | \mathbf{r}'_1 \mathbf{r}'_3 \rangle \Psi_4(\mathbf{r}'_1 \mathbf{r}_2 \mathbf{r}'_3 \mathbf{r}_4) + \text{four further permutations.}$$

Single-nucleon Hamiltonian $\hat{h} = \frac{\hbar^2 p^2}{2m} + [1 - \sum_i^{\text{occ.}} |n\rangle \langle n|] V^{\text{mf}}(r)$

Pauli blocking B $B(1,2) = [1 - f_1(\hat{h}_1) - f_2(\hat{h}_2)]$

Local density approximation: momentum representation, no coupled gradient terms, Thomas-Fermi

Intrinsic motion: in-medium interaction

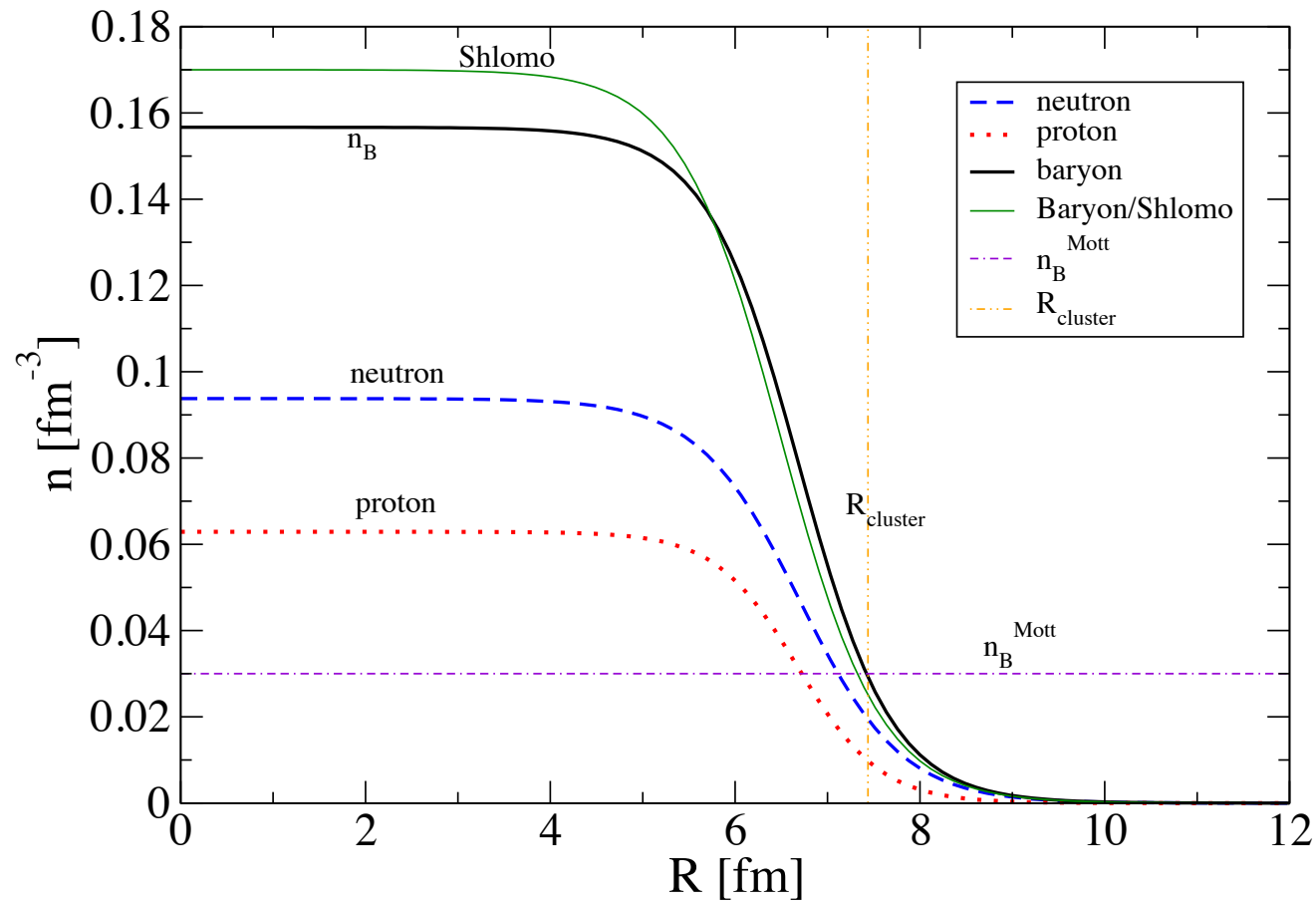
c.o.m. effective potential $W(\mathbf{R}) = W^{\text{ext}}(\mathbf{R}) + W^{\text{intr}}(\mathbf{R}) \quad W^{\text{ext}}(\mathbf{R}) = W^{\text{mf}}(\mathbf{R}) = V_{\alpha-O}^{\text{Coul}}(R) + V_{\alpha-O}^{\text{N-N}}(R)$

$$W^{\text{intr}}(\mathbf{R}) = 4E_F[n_B(\mathbf{R})], \quad E_F(n_B) = (\hbar^2/2m)(3\pi^2 n_B/2)^{2/3}.$$

$$W^{\text{intr}}(\mathbf{R}) = -B_\alpha + W^{\text{Pauli}}[n_B(\mathbf{R})], \quad n_B \leq n_{\text{crit}}$$

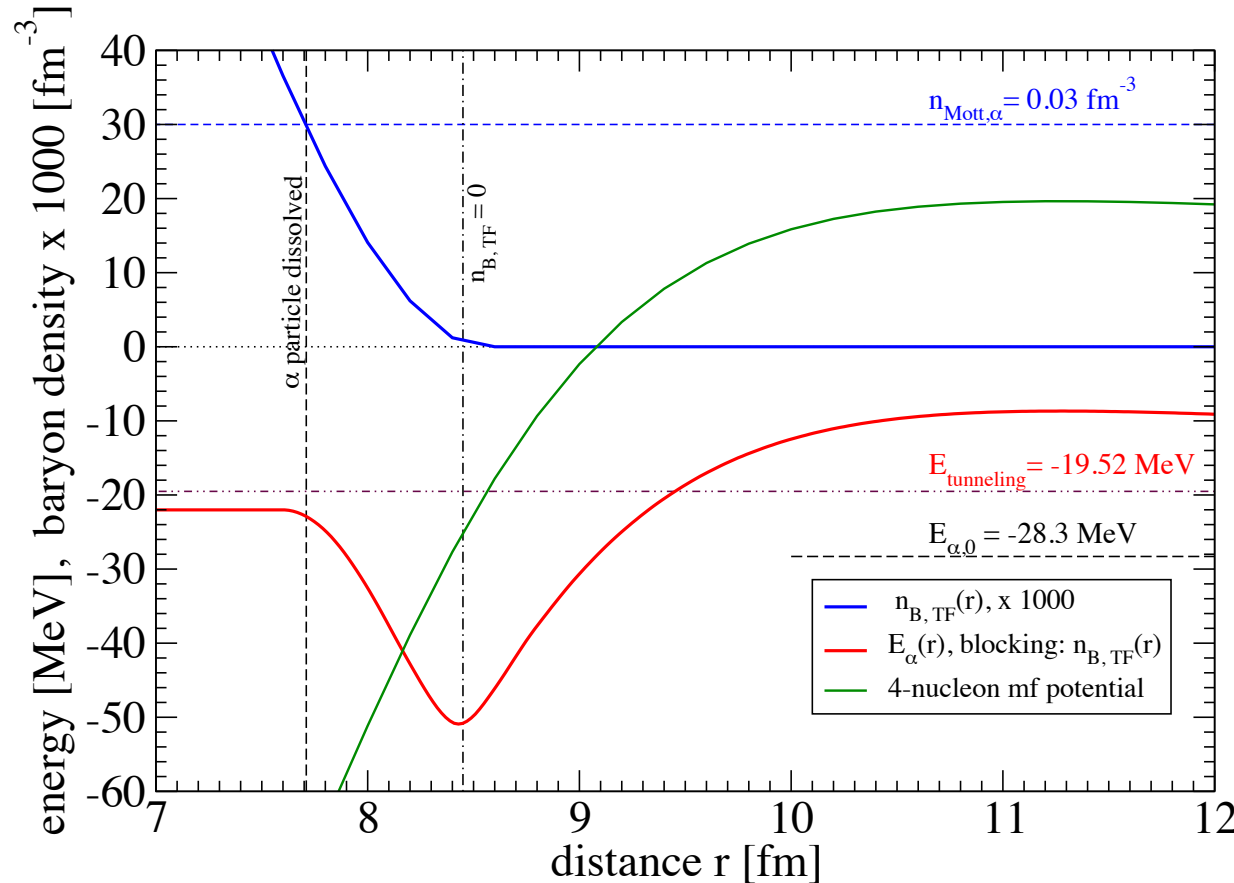
$$W^{\text{Pauli}}(n_B) \approx 4515.9 \text{ MeV fm}^3 n_B - 100935 \text{ MeV fm}^6 n_B^2 + 1202538 \text{ MeV fm}^9 n_B^3$$

Nucleon density of the ^{208}Pb core



^{212}Po : $\alpha(^4\text{He})$ on top of ^{208}Pb

Bound state (quartet) in a dense environment



Coulomb repulsion
+ nuclear attraction
(double folding potential)

density of the lead core

effective potential
of the quartet,
Including intrinsic
(α -like) binding energy

G. R. et al., Physical Review C **90**, 034304 (2014)

C. Xu et al., PRC **93**, 011306(R) (2016)

α decay to doubly magic core in Quartetting
Wave Function Approach ^{104}Te ($\alpha + ^{100}\text{Sn}$):

S. Yang et al., Phys. Rev. C **101**, 024316 (2020)

Nonequilibrium processes

- Heavy ion collisions at Fermi energy conditions (35 MeV per nucleon): fragmentation, nuclear matter phase transition, but expanding fireball, strong nonequilibrium.
- Nucleon-nucleon collisions, Boltzmann (-Uehling-Uhlenbeck) equation (Pauli blocking) for the single-particle distribution function (kinetic equation)
- Formation of bound states: phenomenological coalescence models.
- Reaction kinetics: Thermonuclear reaction networks for astrophysics (SN)
- Formation of hot and dense matter (equilibrium), energy dissipation
- expansion: hydrodynamics (local thermodynamic equilibrium), flow
- Freeze-out of the equilibrium distribution, feed-down (decay of excited states, afterburner)
- Reconstruction of the initial state from final yields (statistical models, temperature and density as parameters to describe the distribution of clusters)
- Ultrarelativistic heavy-ion collisions
- Fission (ternary fission)
- Cosmology: nucleosynthesis

Relevant statistical operator

State of the system in the past $\text{Tr}\{\rho(t)B_n\} = \langle B_n \rangle^t$

Construction of the relevant statistical operator at time t

$$S_{\text{rel}}(t) = -k_B \text{Tr}\{\rho_{\text{rel}}(t) \log \rho_{\text{rel}}(t)\} \rightarrow \text{maximum}$$

$$\delta[\text{Tr}\{\rho_{\text{rel}}(t) \log \rho_{\text{rel}}(t)\}] = 0$$

$$\text{Tr}\{\rho_{\text{rel}}(t)B_n\} \equiv \langle B_n \rangle_{\text{rel}}^t = \langle B_n \rangle^t$$

Generalized Gibbs distribution

$$\rho_{\text{rel}}(t) = \exp\left\{-\Phi(t) - \sum_n \lambda_n(t)B_n\right\}$$

equations of state to eliminate $\lambda_n(t)$

$$\Phi(t) = \log \text{Tr} \exp\left\{-\sum_n \lambda_n(t)B_n\right\}$$

$$\frac{\partial S_{\text{rel}}(t)}{\partial t} = \sum_n \lambda_n(t) \langle \dot{B}_n \rangle^t$$

But: von Neumann equation?

Entropy?

Nonequilibrium statistical operator (NSO)

principle of weakening of initial correlations (Bogoliubov, Zubarev)

$$\rho_\epsilon(t) = \epsilon \int_{-\infty}^t e^{\epsilon(t_1-t)} U(t, t_1) \rho_{\text{rel}}(t_1) U^\dagger(t, t_1) dt_1$$

time evolution operator $U(t, t_0)$ relevant statistical operator $\rho_{\text{rel}}(t)$

selection of the set of relevant observables $\{B_n\}$

self-consistency relations $\text{Tr}\{\rho_{\text{rel}}(t) B_n\} \equiv \langle B_n \rangle_{\text{rel}}^t = \langle B_n \rangle^t$

maximum of information entropy $S_{\text{rel}}(t) = -k_B \text{Tr}\{\rho_{\text{rel}}(t) \log \rho_{\text{rel}}(t)\}$

generalized Gibbs distribution $\rho_{\text{rel}}(t) = \exp\left\{-\Phi(t) - \sum_n \lambda_n(t) B_n\right\}$

von Neumann equation

$$\frac{\partial}{\partial t} \rho_\epsilon(t) + \frac{i}{\hbar} [H, \rho_\epsilon(t)] = -\epsilon (\rho_\epsilon(t) - \rho_{\text{rel}}(t))$$
$$\rho(t) = \lim_{\epsilon \rightarrow 0} \rho_\epsilon(t)$$

Expanding nuclear matter: freeze-out and reaction processes (feed-down)

EoS at low densities from HIC

PRL 108, 172701 (2012)

PHYSICAL REVIEW LETTERS

week ending
27 APRIL 2012

Laboratory Tests of Low Density Astrophysical Nuclear Equations of State

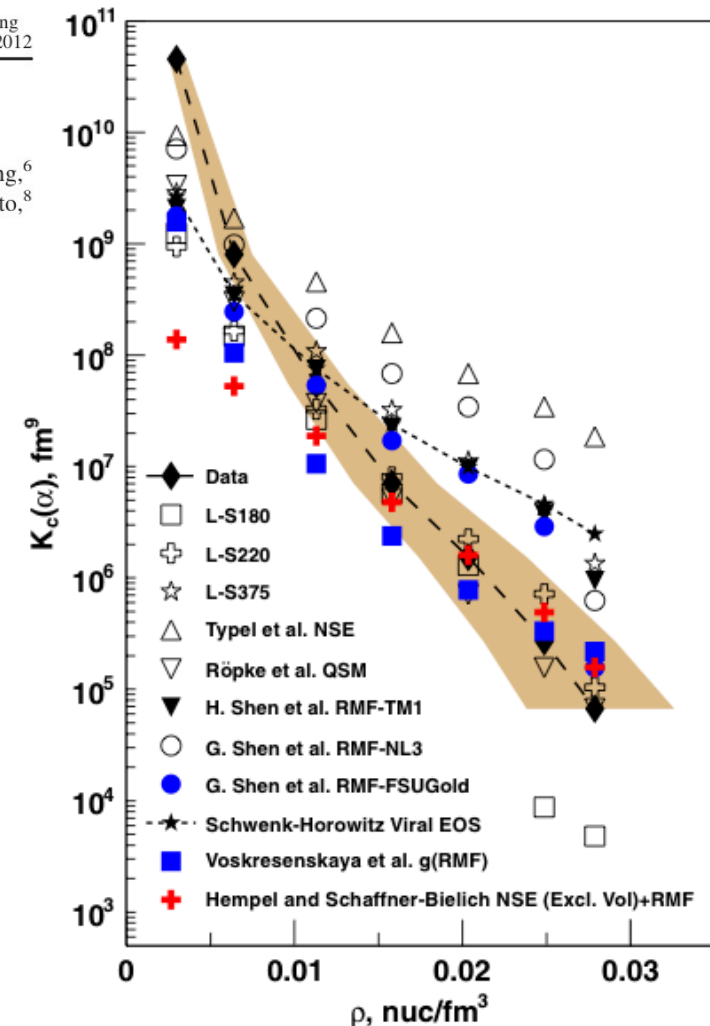
L. Qin,¹ K. Hagel,¹ R. Wada,^{2,1} J. B. Natowitz,¹ S. Shlomo,¹ A. Bonasera,^{1,3} G. Röpke,⁴ S. Typel,⁵ Z. Chen,⁶ M. Huang,⁶ J. Wang,⁶ H. Zheng,¹ S. Kowalski,⁷ M. Barbui,¹ M. R. D. Rodrigues,¹ K. Schmidt,¹ D. Fabris,⁸ M. Lunardon,⁸ S. Moretto,⁸ G. Nebbia,⁸ S. Pesente,⁸ V. Rizzi,⁸ G. Viesti,⁸ M. Cinausero,⁹ G. Prete,⁹ T. Keutgen,¹⁰ Y. El Masri,¹⁰ Z. Majka,¹¹ and Y. G. Ma¹²

Yields of clusters from HIC: p, n, d, t, h, α

chemical constants

$$K_c(A, Z) = \rho_{(A,Z)} / [(\rho_p)^Z (\rho_n)^N]$$

inhomogeneous,
non-equilibrium



Generalized RMF

$$\mathcal{L} = \sum_{j=n,p,d,t,h,\alpha} \mathcal{L}_j + \mathcal{L}_\sigma + \mathcal{L}_\omega + \mathcal{L}_\rho + \mathcal{L}_{\omega\rho}$$

Effective Lagrangian:
quasiparticle nuclei as
new degrees of freedom

$$M_j^* = A_j m - g_{sj} \phi_0 - (B_j^0 + \delta B_j).$$

Coupling to the meson fields
depending on A

$$g_{sj} = x_{sj} A_j g_s$$

$$x_{sj} = 0.85 \text{ for } A > 1$$

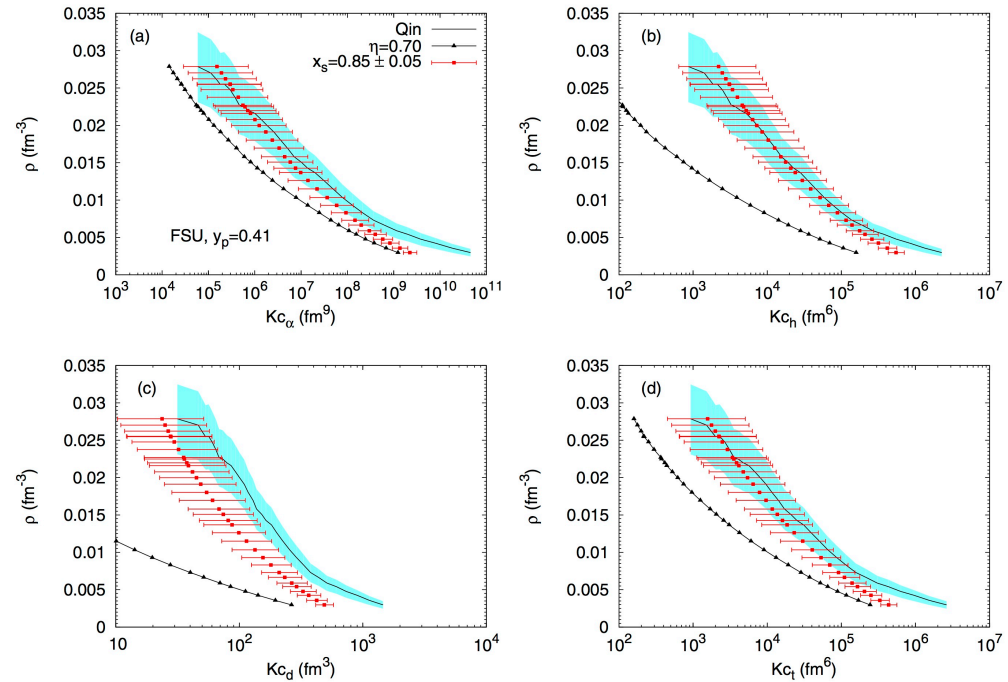


FIG. 7. Chemical equilibrium constants of α (a), helion (b), deuteron (c), and triton (d) for FSU, and $y_p = 0.41$, and for the $\eta = 0.70$ (black squares) fitting (check Ref. [17] for the complete parameter sets) and the universal g_{sj} fitting with $g_{sj} = (0.85 \pm 0.05) A_j g_s$, (red dotted lines). The experimental results of Qin *et al.* [18] (light blue region) are also shown.

Including light clusters to the EoS

Eur. Phys. J. A (2020) 56:295
<https://doi.org/10.1140/epja/s10050-020-00302-w>

THE EUROPEAN
 PHYSICAL JOURNAL A



Regular Article - Theoretical Physics

Light clusters in warm stellar matter: calibrating the cluster couplings

Tiago Custódio¹, Alexandre Falcão¹, Helena Pais^{1,a}, Constança Providência¹, Francesca Gulminelli², Gerd Röpke^{3,4}

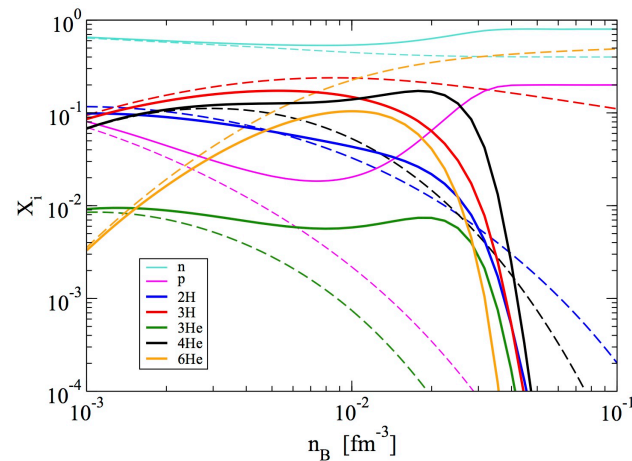


Fig. 1 The abundances (mass fraction) of the stable isotopes n , p , d , t , h , α , and ${}^6\text{He}$ considered as a function of the density for $T = 5$ MeV and a fixed proton fraction of 0.2. The NSE (dashed) is compared to a QS calculation (full lines), see text

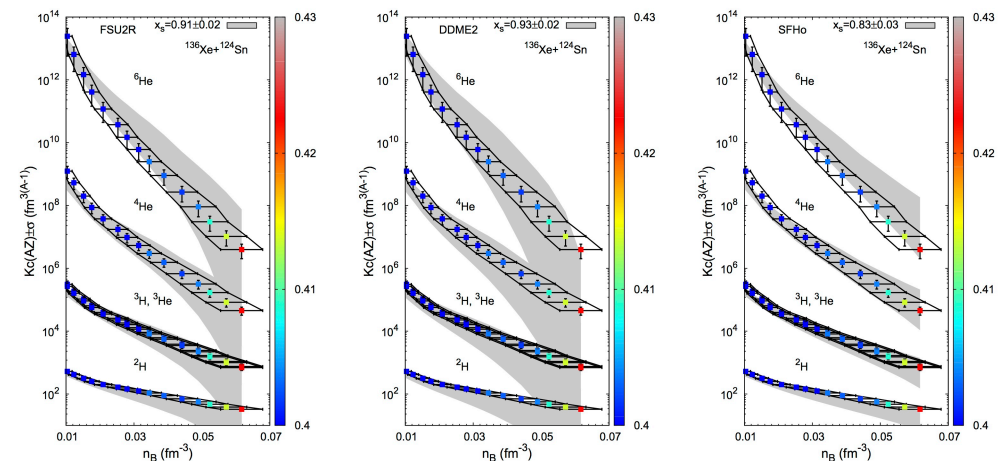


Fig. 6 The equilibrium constants as a function of the density. The full lines represent the experimental results of the INDRA collaboration, with 1σ uncertainty. The grey bands are the equilibrium constants from a calculation [30] where we consider homogeneous matter with five light clusters for the FSU2R EoS (left), the DDME2 EoS (middle) and

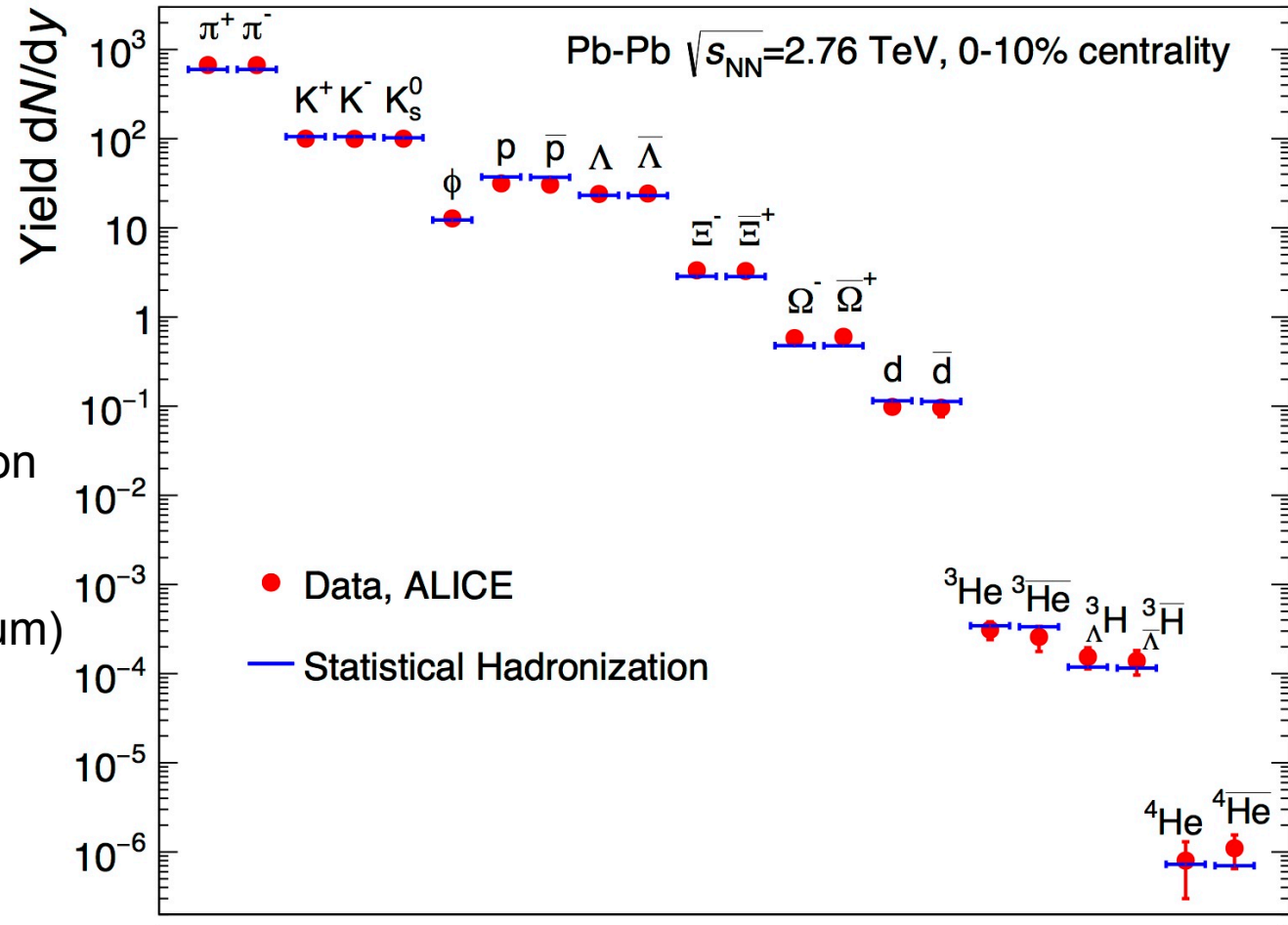
SFHo EoS (right), calculated at the average value of $(T, n_{B,\text{exp}}, y_{p,\text{exp}})$, and considering cluster couplings in the range of $x_s = 0.91 \pm 0.02$ (FSU2R), $x_s = 0.93 \pm 0.02$ (DDME2) and $x_s = 0.83 \pm 0.03$ (SFHo). The color code represents the global proton fraction

Cluster formation at LHC/CERN

ALICE@LHC

Excellent description
Of data by the
Statistical model
(chemical equilibrium)

$T = 156 \text{ MeV}$



A. Andronic, P. Braun-Munzinger, K. Redlich, J. Stachel, Nature 561, 321 (2018)

Density effects?

The Beth-Uhlenbeck equation is identical
with the Dashen, Ma, Bernstein approach.

Talk given by Peter Braun-Munzinger:

the proton anomaly and the Dashen, Ma, Bernstein S-matrix approach

thermal yield of an
(interacting) resonance
with mass M , spin J , and
isospin I

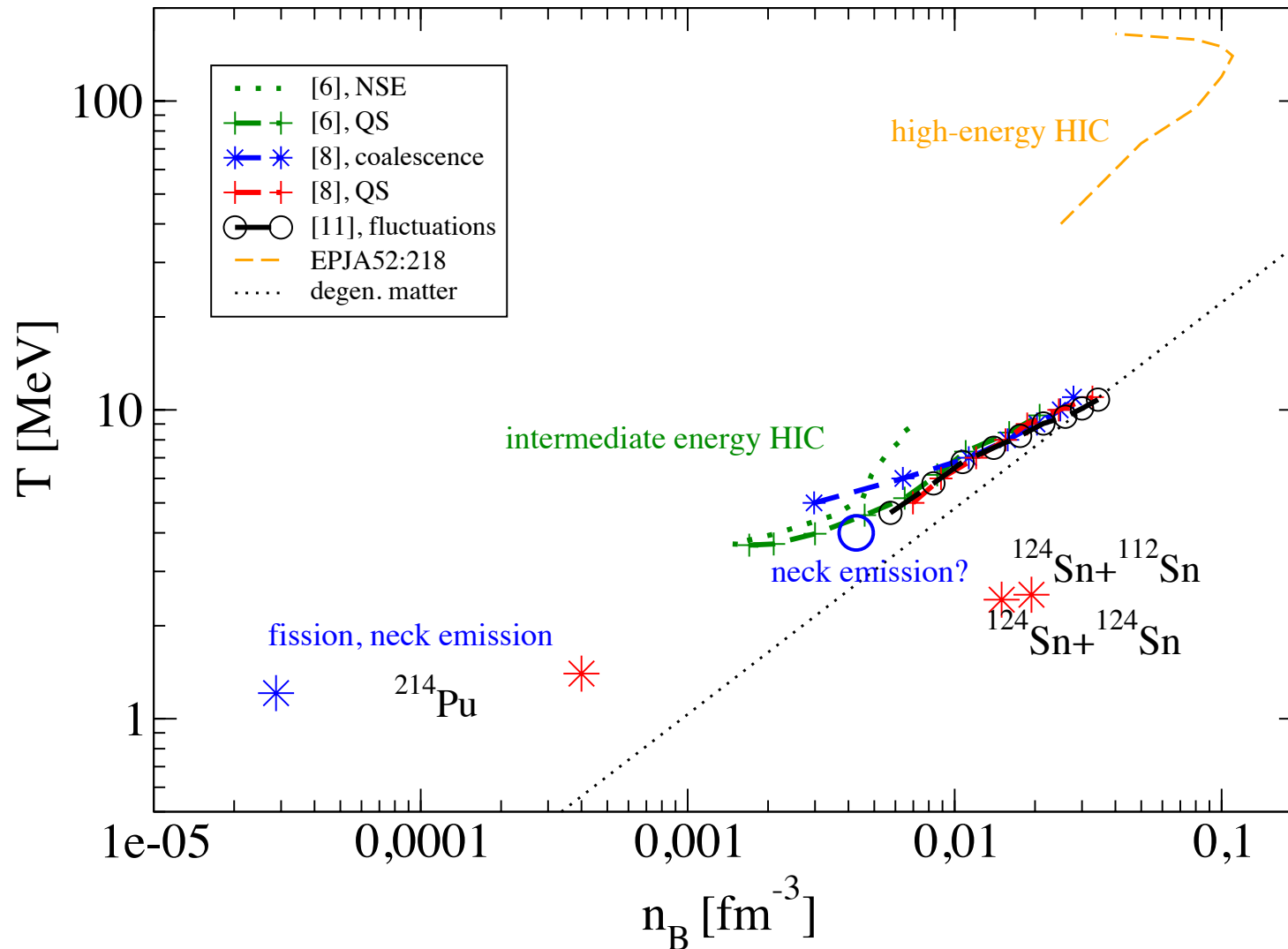
$$\langle R_{I,J} \rangle = d_J \int_{m_{th}}^{\infty} dM \int \frac{d^3p}{(2\pi)^3} \frac{1}{2\pi} B_{I,J}(M) \\ \times \frac{1}{e^{(\sqrt{p^2+M^2}-\mu)/T} + 1},$$

need to know derivatives
of phase shifts with
respect to invariant mass

$$B_{I,J}(M) = 2 \frac{d\delta_J^I}{dM}.$$

A. Andronic, pbm, B. Friman,
P.M. Lo, K. Redlich, J. Stachel,
arXiv:1808.03102,
Phys.Lett.B792 (2019)304

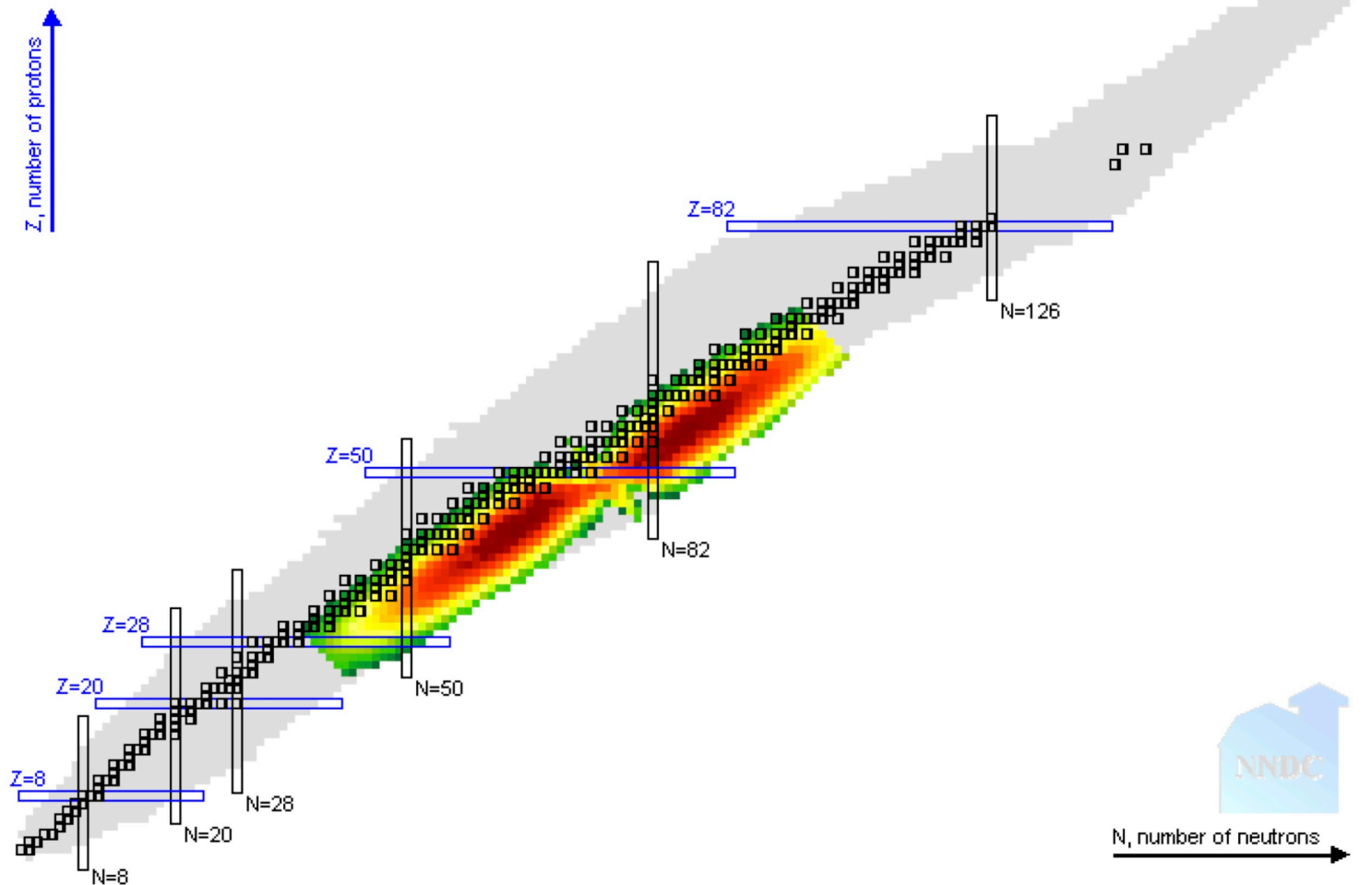
Freeze-out temperatures and densities



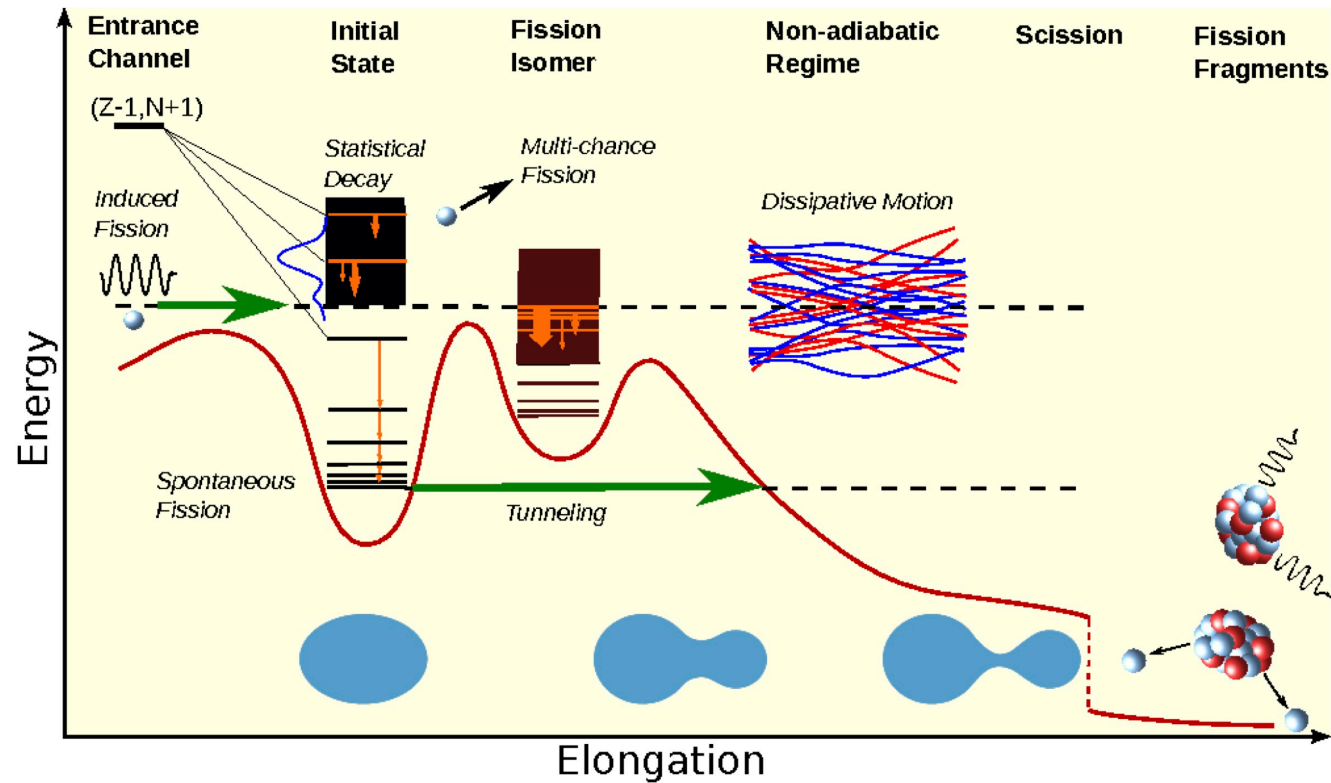
Spontaneous fission of actinides

Nudat 2.8: ^{252}Cf

Distribution of fission fragments



Nuclear Fission

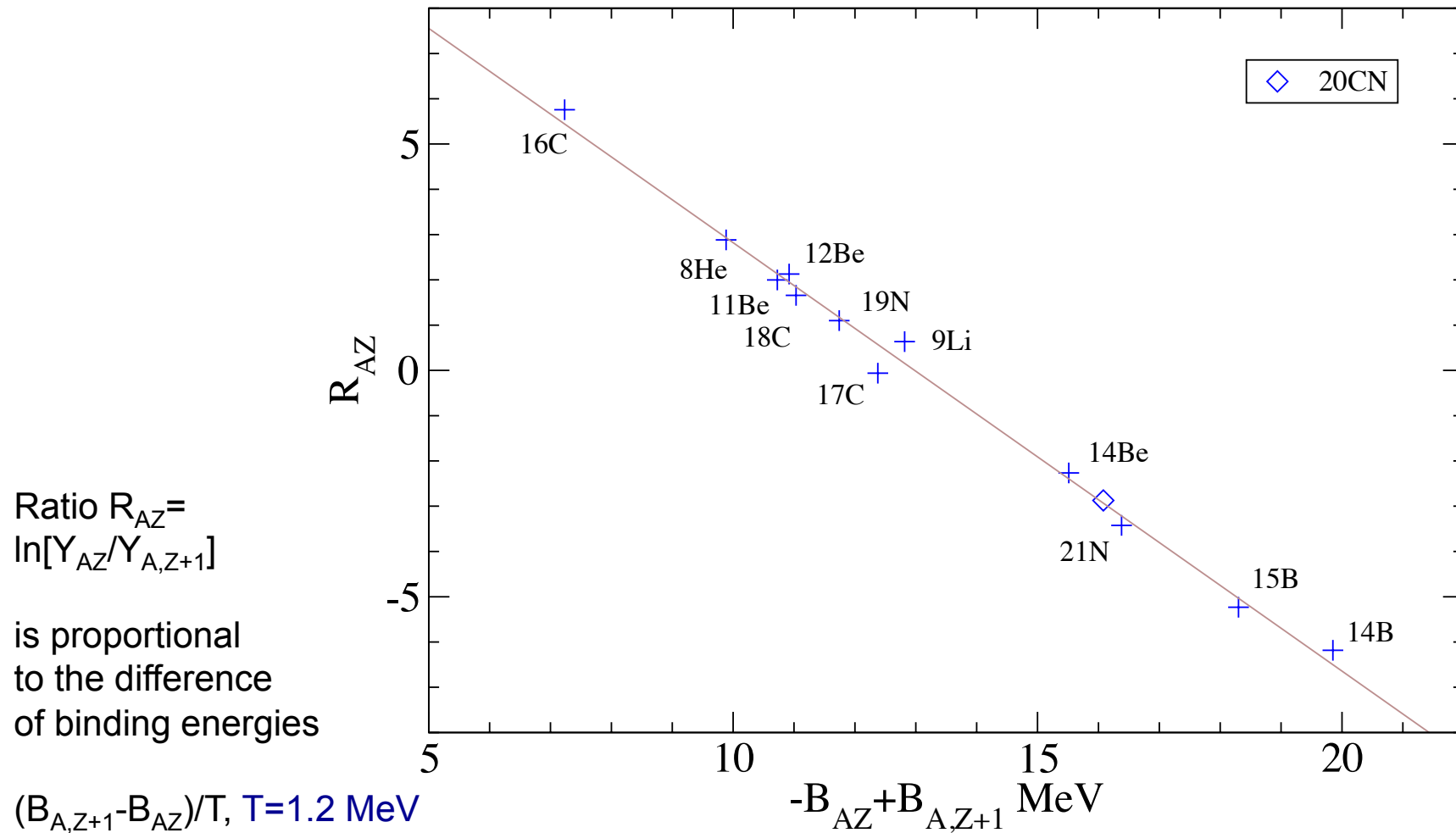


quadrupole fluctuations (GDR)
tunneling – deformed droplets, neck formation

Future of Nuclear Fission Theory

M. Bender et al., J. phys. G: Nucl. Part. Phys. 47, 113002 (2020)

Ternary fission: light cluster yields



Fission: yields of H and He isotopes

Nonequilibrium information entropy approach to ternary fission of actinides

isotope	$R_{A,Z}^{\text{vir}}$	$^{233}\text{U}(n_{\text{th}},f)$	$^{235}\text{U}(n_{\text{th}},f)$	$^{239}\text{Pu}(n_{\text{th}},f)$	$^{241}\text{Pu}(n_{\text{th}},f)$	$^{248}\text{Cm}(sf)$	$^{252}\text{Cf}(sf)$
λ_T [MeV]	1.3	1.24177	1.21899	1.3097	1.1900	1.23234	1.25052
λ_n [MeV]	-	-3.52615	-3.2672	-3.46688	-3.02055	-2.92719	-3.1107
λ_p [MeV]	-	-15.8182	-16.458	-16.2212	-16.6619	-16.7798	-16.7538
^1_0n	-	560012	1.409e6	722940	1.8579e6	1.606e6	1.647e6
^1_1H	-	28.131	28.16	42.638	19.52	21.079	30.096
$^2\text{H}^{\text{obs}}$	-	41	50	69	42	50	63
^2H	0.973	40.986	49.76	68.632	41.563	49.533	61.579
$^3\text{H}^{\text{obs}}$	-	460	720	720	786	922	950
^3H	0.998	457.27	715.29	714.79	780.39	913.76	943.12
^4H	0.0876	2.7772	4.97	5.627	6.057	8.742	8.219
^3He	0.997	0.0124	0.0076	0.0235	0.00431	0.00645	0.00933
$^4\text{He}^{\text{obs}}$	-	10000	10000	10000	10000	10000	10000
^4He	1	8858.46	8706.1	8615.7	8556.9	8313.98	8454.0
^5He	0.689	1130.75	1289.04	1374.7	1439.0	1680.75	1540.9
$^6\text{He}^{\text{obs}}$	-	137	191	192	260	354	270
^6He	0.933	115.89	158.98	159.01	211.68	276.96	222.4
^7He	0.876	21.262	33.997	35.983	51.742	80.634	58.16
$Y_{^6\text{He}}^{\text{obs}}/Y_{^6\text{He}}^{\text{final, vir}}$	-	0.9989	0.9897	0.9846	0.9869	0.9899	0.9622
$^8\text{He}^{\text{obs}}$	-	3.6	8.2	8.8	15	24	25
^8He	0.971	3.4725	6.764	6.4095	12.481	21.280	13.32
^9He	0.255	0.047077	0.105	0.111	0.219	0.455	0.258
$Y_{^8\text{He}}^{\text{obs}}/Y_{^8\text{He}}^{\text{final, vir}}$	-	1.0229	1.1936	1.3496	1.1811	1.1042	1.8409
^8Be	1.07	5.7727	2.594	5.147	2.188	2.819	2.544

Lagrange parameters

observed yields,

primary yields,
virial partition function

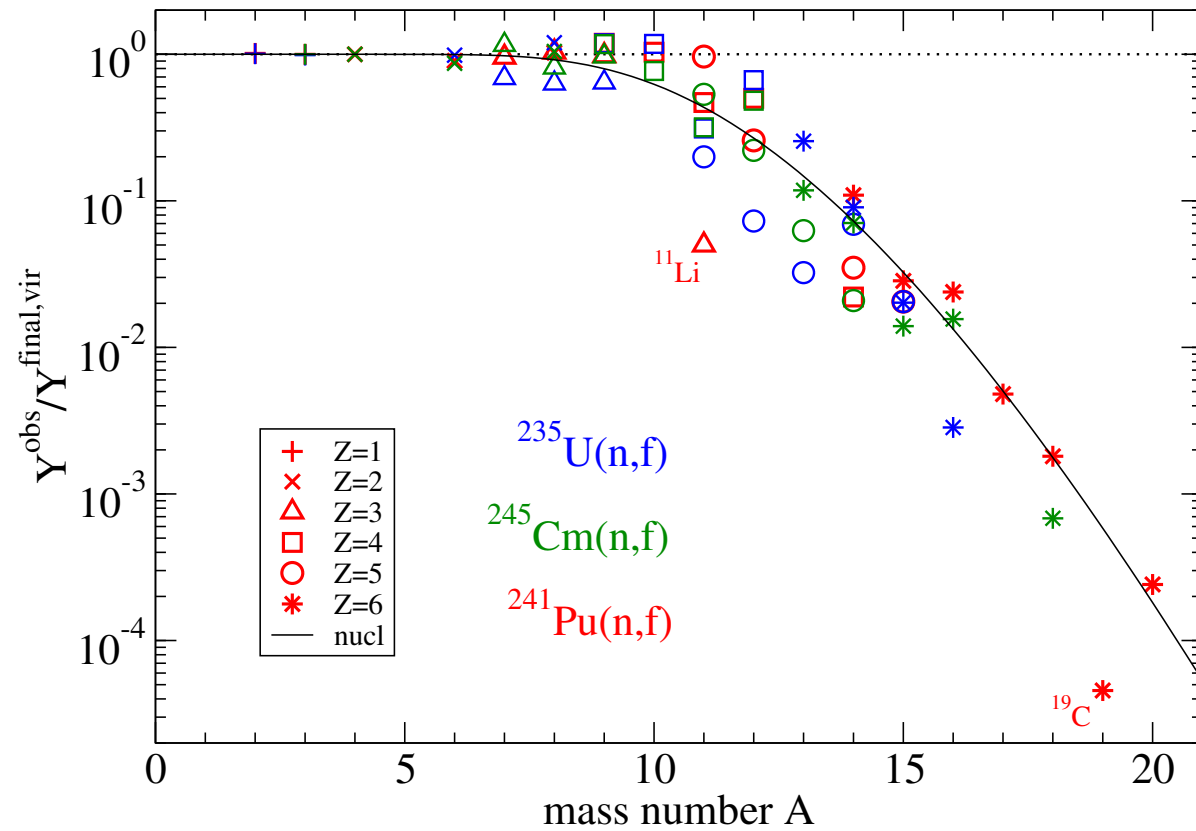
intrinsic partition function,
no density corrections:

^6He is overestimated,
 ^8He is underestimated:

Pauli blocking?

G.R., J. B. Natowitz, H. Pais, Phys. Rev. C 103, L061601 (2021)

Larger clusters: nucleation kinetics?

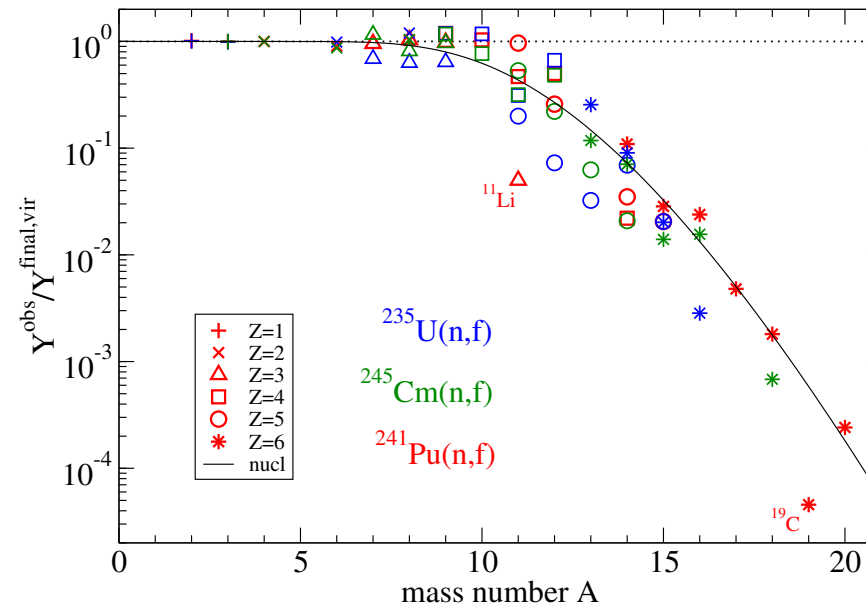


Ternary fission: light cluster yields

Neck formation and scission: freeze-out, low-density neutron-rich matter

Nonequilibrium information entropy approach to ternary fission of actinides

$T = 1.24 \text{ MeV}$
 $\mu_n = -2.99 \text{ MeV}$
 $\mu_p = -16.35 \text{ MeV}$
 $n_B = 0.000067 \text{ fm}^{-3}$
 $Y_p = 0.035$



nucleation kinetics

$$Y_{A,Z}^{\text{obs}} / Y_{A,Z}^{\text{final,vir}} = \frac{1}{2} \text{erfc} \left[b(\tau) (A^{1/3} - a(A_c, \tau)) \right]$$

saddle-to-scission relaxation time about 7000 fm/c

size effect?

Solar element abundances

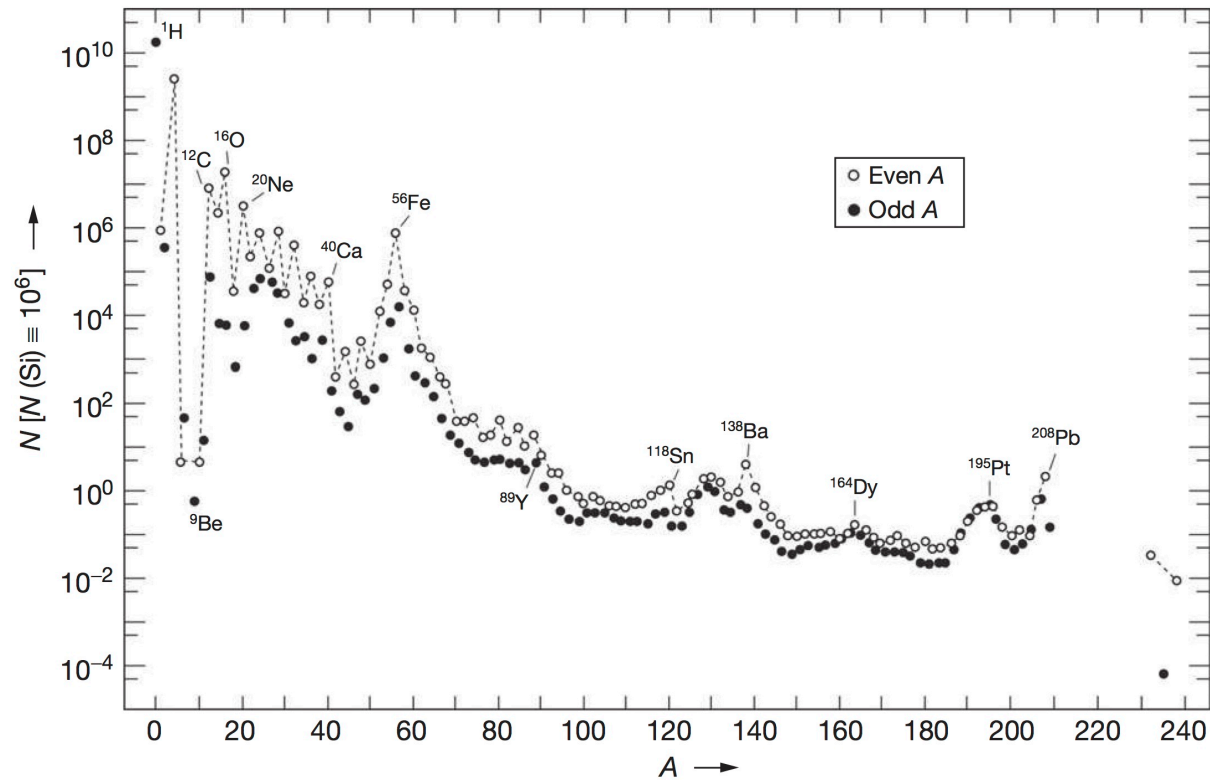


Figure 7 Solar system abundances by mass number. Atoms with even masses are more abundant than those with odd masses (Oddo–Harkins rule). There is no smooth dependence of abundances on mass numbers for even (e.g., ${}^{118}\text{Sn}$ and ${}^{138}\text{Ba}$) or for odd masses (e.g., ${}^{89}\text{Y}$).

H. Palme, K. Lodders, A. Jones, *Solar System Abundances of the Elements* (Elsevier 2014)

Gross structure of cluster distribution

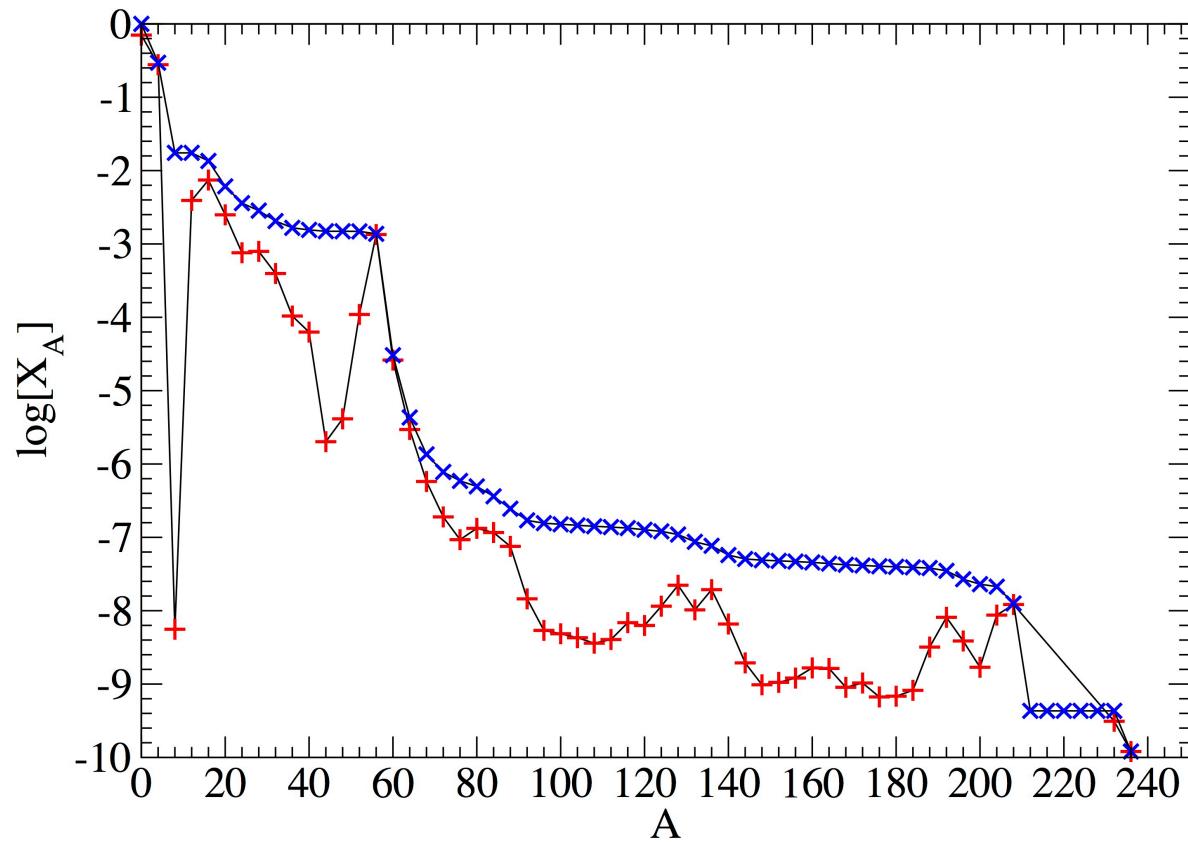
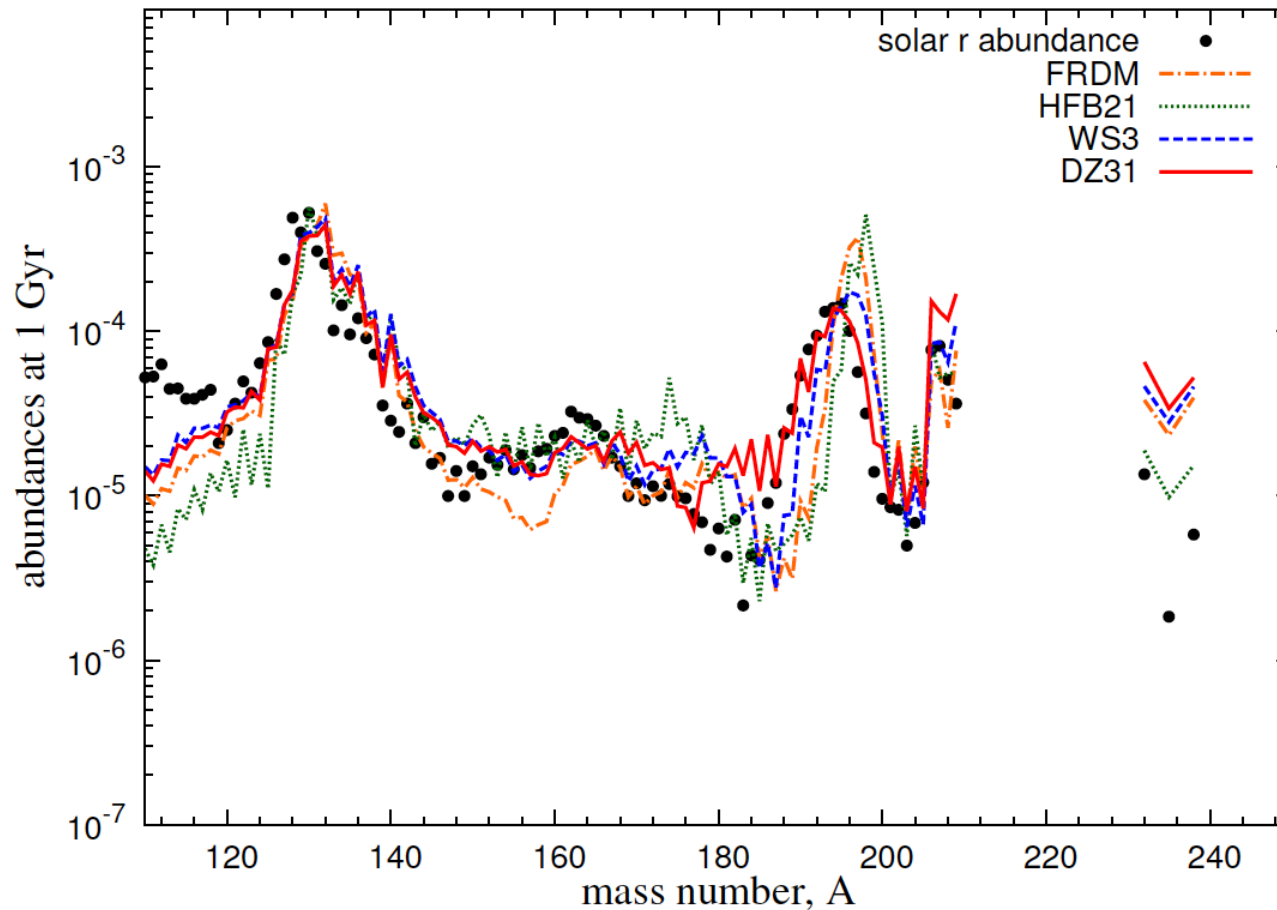


FIG. 1. Accumulated mass fraction $\hat{X}_{\hat{A}} = \sum_{A'=\hat{A}}^{\hat{A}+3} A' \sum_{Z,\nu} n_{A',Z,\nu} / n_b$ and the \hat{A} -metallicity $M_{\hat{A}} = \sum_{A' \geq \hat{A}} \hat{X}_{A'}$. Data from Lodders [4], see Tabs. I, II.

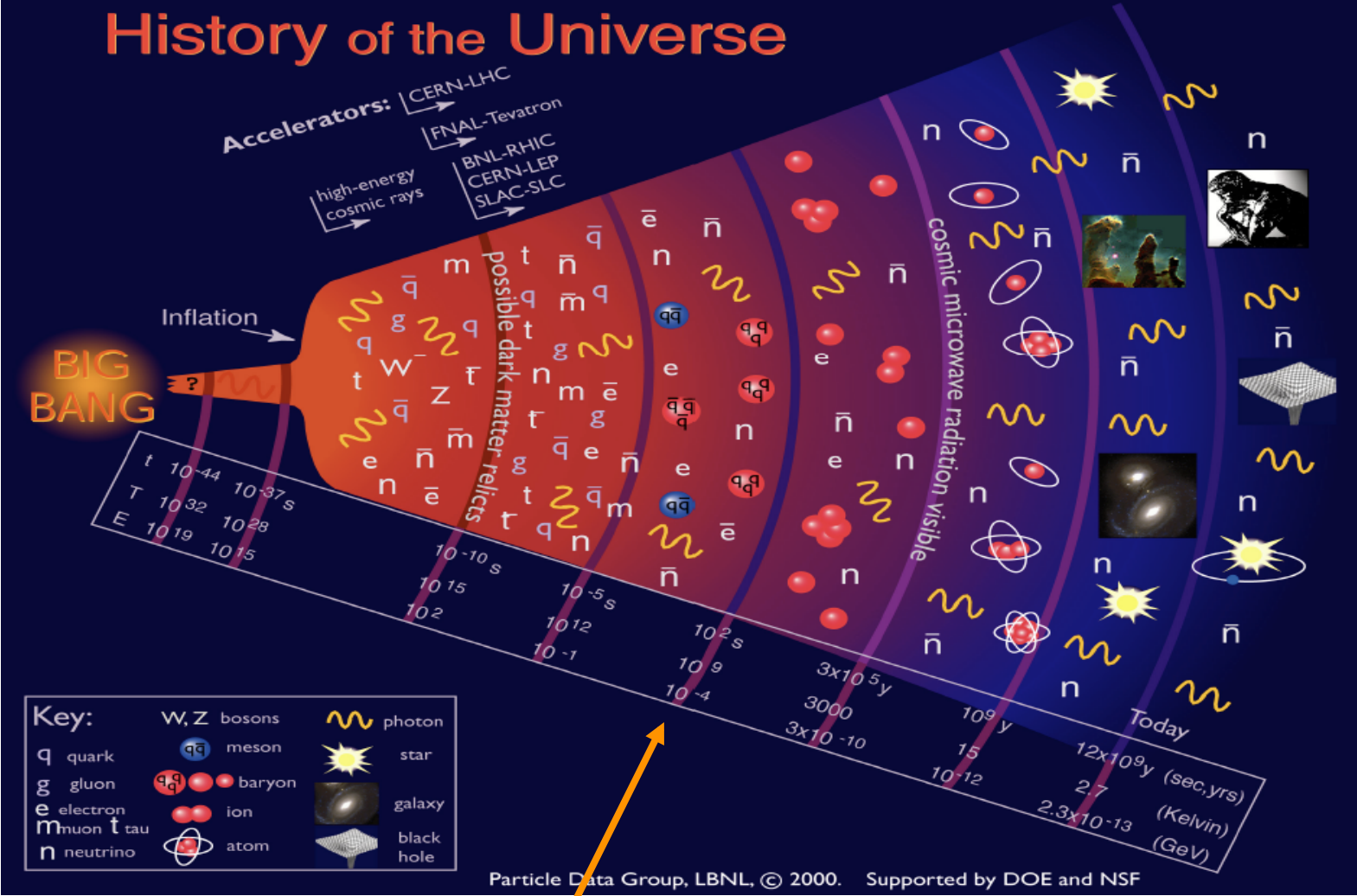
Neutron star merger simulation



Final mass-integrated r-process abundances obtained in a neutron star merger simulation using four different mass models compared to solar system r-process abundances [Mendoza-Temis et al. PRC 92 (2015) 055805].

J. Cowan, C. Sneden, J.E. Lawler, A. Aprahamian, M. Wiescher, K. Langanke, G. Martinez-Pinedo, F.-K. Thielemann: "Making the heaviest elements in the Universe: A review of the rapid neutron capture process", arxiv:1901.01410

Origin of chemical elements



Big-Bang nucleosynthesis, time ~ 100 sec, temperature $\sim 10^9$ K